A. G. Shtukenberg, B. Kahr et al.

DOI: 10.1002/anie.201301223

Crystal Growth

Growth Actuated Bending and Twisting of Single Crystals

Alexander G. Shtukenberg, Yurii O. Punin, Ankit Gujral, and Bart Kahr**

Keywords:
crystal growth · electron microscopy · helical structures · mechanical properties · X-ray diffraction

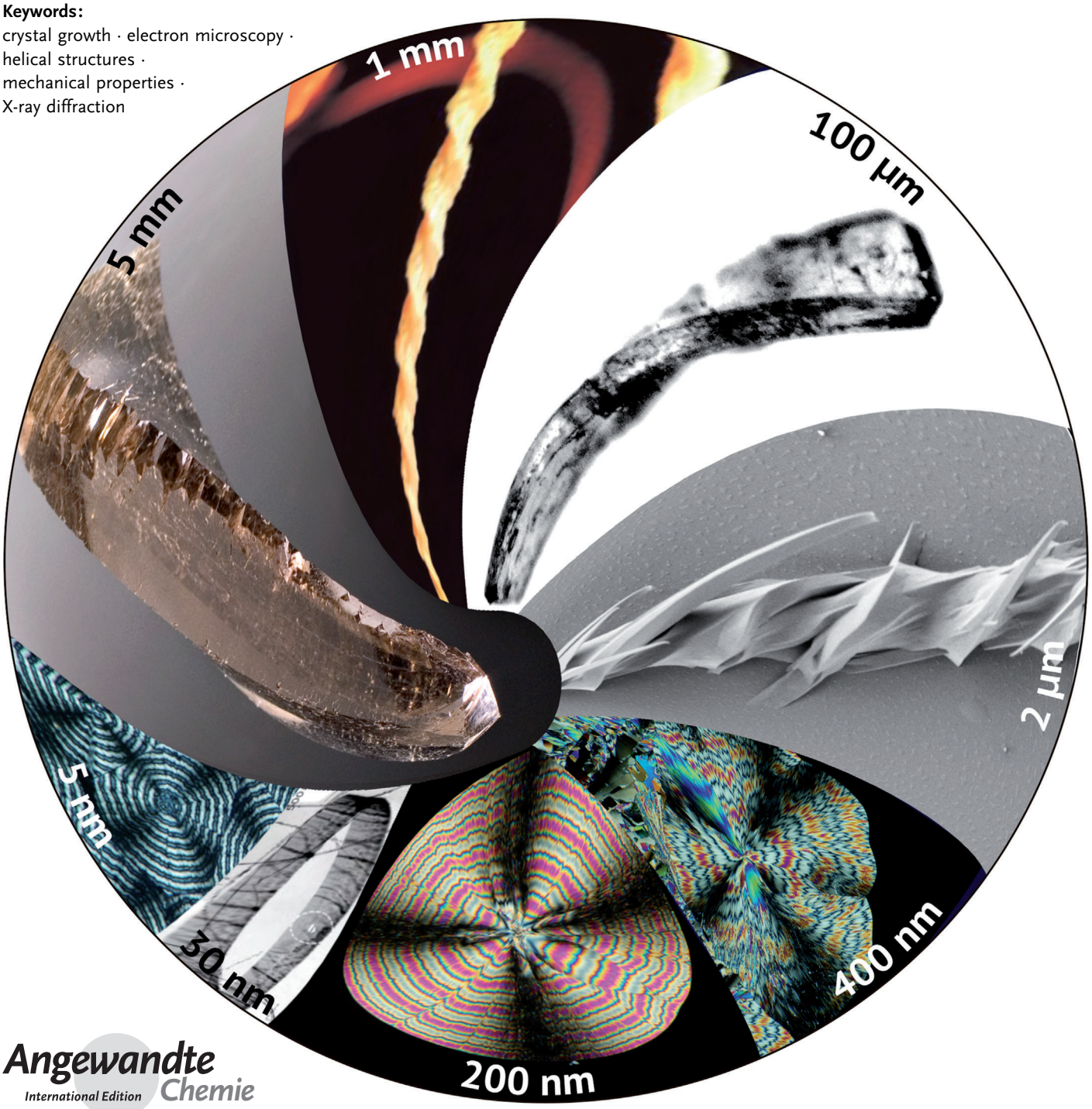

Crystals of a variety of substances including elements, minerals, simple salts, organic molecular crystals, and high polymers forgo long-range translational order by twisting and bending as they grow. These deviations have been observed in crystals ranging in size from nanometers to centimeters. How and why so many materials choose dramatic non-crystallographic distortions is analyzed, with an emphasis on crystal chemistries that give rise to stresses operating either on surfaces of crystallites or within the bulk.

> *"Thus the whale-line folds the whole boat in its complicated coils, twisting and writhing around it in almost every direction."*
> Herman Melville, Moby Dick, Chapter 60

From the Contents

1. Introduction

In 1929, Ferdinand Bernauer (1890–1945) concluded that about one quarter of simple molecular crystals can be made to grow as mesoscale helices.[1] Bernauer's judgment was based on analyses of the optical properties and morphologies of more than 400 melt-grown crystals of substances that he was able to obtain from colleagues throughout Germany. His far-reaching judgment about crystal morphology, of which recent monographs on crystal growth say not a word,[2–5] has changed our view of crystals and crystallography. After some study, we now know Bernauer's claim to be true.[6]

One of the substances studied by Bernauer, hippuric acid (*N*-benzoylglycine), grows from slightly undercooled melts as flat ribbons (Figure 1 a). Between crossed polarizers, the ribbons of uniform thickness show a remarkable progression of dark bands that correspond to outcrops of optic axes that arise as the lattice smoothly rotates about the perpendicular to the optic plane.[7,8] The helically turning optical indicatrix (an ellipsoidal surface whose radii are in proportion to the refractive indices and defines the refraction anisotropy) appears to be projected onto the planar ribbon. Hippuric acid crystals, when grown from the vapor, are not constrained as in a melt between glasses, and curve freely as shown in Figure 1 b. Hippuric acid seems peculiar. But, it is our aim herein to normalize crystallographic oddities of this kind.

Most of the twisted crystals studied by Bernauer are so-called ring-banded spherulites (Figure 1) of simple molecular substances. (Hippuric acid also forms ring-banded spherulites (Figure 1 e) in addition to the isolated ribbons in Figure 1 a,b)[6] Spherulites are radial aggregates of fibrous crystals with round interfaces at sufficiently large length scales.[12] A typical ring-banded spherulite grown by Bernauer is of aspirin (acetylsalicylic acid).[13] The concentric bands of extinction in Figure 1 c suggesting modulated optical properties are a telltale sign of twisting. The optical bands correspond to periodic and continuous changes in crystallite orientation from edge-on to flat-on lamellae(Figure 2).

While ring-banded spherulites have been a focus of our work, and also of Bernauer's, on twisted crystals, there are, in fact, many crystalline products of nature and the laboratory with curved lattices. In this Review, we restrict ourselves to single crystals that are characterized by growth-induced bending and twisting of the crystal lattice.

The concepts of crystal and non-planar (*hkl*) "planes", may seem incompatible. In an unbounded crystal, an integral number of translations along three non-coplanar vectors $\mathbf{a}_1$, $\mathbf{a}_2$, $\mathbf{a}_3$ brings us to a position that is precisely equivalent in structure and in potential energy. This is not so in twisted hippuric acid (Figure 1 a,b,e), or aspirin (Figure 1 c, Figure 2), or in many other simple crystalline substances, a great fraction of which spontaneously grow so as to subvert the very definition of crystal. But, real crystals are imperfect and can only approximate mathematical objects. Real crystals contain defects, dislocations, and disclinations that distort lattices locally, however, they may cooperate to bend and twist crystals globally.

In advance of discussing growth-distorted crystal morphologies, we will first specify some crystalline objects that we exclude from this Review. Among these exclusions are single crystals with curved faces but straight lattices. Such crystals commonly arise through thermal surface roughening,[14] the development of pronounced vicinal facets,[15] or the action of strongly adsorbing impurities.[16–18] Spencer reminds us that the mineralogist's vocabulary is loaded with soft adjectives not easily applied to polyhedra including the following: globular, botryoidal, mammiform, reniform, warty, nodular, amygdaloidal, stalactitic, coralloidal, vermicular, dendritic, arborescent, wiry, mossy, and plumose.[19]

We also exclude post-growth deformations of crystals in this Review about crystal growth processes. Earth pressures

[*] Dr. A. G. Shtukenberg, A. Gujral, Prof. B. Kahr
Department of Chemistry and Molecular Design Institute
New York University
100 Washington Square East, Room 1001
New York City, NY 10003 (USA)
E-mail: shtukenberg@mail.ru
bart.kahr@nyu.edu
Prof. Y. O. Punin
Department of Crystallography, Geological Faculty
St. Petersburg State University
Universitetskaya emb., 7/9, St. Petersburg 199034 (Russia)

can bend and twist minerals.[20] Where there is a force, there will naturally be a response. Recent spectacular examples of photochemically distorted crystals include substances that undergo pericyclic reactions thus producing heterometries—metric differences in subvolumes of the crystal—that create strain-induced stresses which in turn affect macroscopic distortions.[21–24] Potassium salts of 3,4,9,10-perylenetetracarboxylic acid grow as straight ribbons, but twist and coil when dispersed in fluids that differentially solvate surfaces.[25] InSb shows spontaneous bending in annealed thin slices perpendicular to a polar axis.[26] Fascinating as is the materials science in the aforementioned examples, the associated substances fall outside our set of twisted crystals.

Almost every crystal growing from the melt can be bent by an inhomogeneous temperature distribution followed by thermoelastic and thermoplastic stress.[14,27] High plasticity near the melting point facilitates deformations. Ice dendrites on a glass window in winter—a quintessential image of cold—may actually curve thermoplastically.[28] Although this trivial phenomenon is not considered herein, it is not wholly unrelated to real twisted crystals as we will show in Section 5.5.

We also exclude curved aggregates of small straight-edged crystals (Section 6.1). Helical mesocrystals[29] are described with increasing frequency in the literature. They are only superficially related in form to continuously twisted crystals. Imai and Oaki[30] have recently illustrated helical ensembles in a number of substances including aspartic acid.[31] The segmented quality of the structures is unequivocal in the scanning electron micrographs (SEMs) shown in Figure 3. We must necessarily be mindful of helical ensembles throughout because it may well be that the segments correspond to the independent growth of crystallites emanating from a helically twisted core.

Chemistry is replete with structured bent and helical ensembles that give discrete diffraction patterns that occupy intermediate positions between classical crystals and supramolecular ensembles.[33–39] Highly crystalline amyloid and tau protein[40] fibrils (Figure 4a) associated with neurodegeneracies fall within this class. They are composed of twisted, multilayered β-sheet lamellae just 20 nm across. Do they belong in this Review? We presume that for a crystal to be bent or twisted (note the past tense, twisted not twist) it must have an analogous undistorted structure with long-range translational symmetry and conforming to one of the 230 traditional Federov–Shoenflies space groups. (We have yet to learn of a twisted quasicrystal, but they are undoubtedly possible.) Regarding the twisted silk fibroin (Figure 4b),[41] we can anticipate, on the basis of our accumulated knowledge of the crystal kingdom, that there could and should be an untwisted form with a well-defined space group.[42] The polyphenylacetylene with cyclodextrin pendants in Figure 4c makes double helices of helical tubules that are as large as 6 μm in radius.[43] But, this is surely best described as a complex supramolecular rope, albeit large and periodic. Cholic acid helices have a high degree of crystallinity evident in powder X-ray scattering experiments, supporting comparisons with twisted crystals,[44] but morphologically they are aggregates. On the other hand, 10,12-tricosadynoic anhydride deposits helically twisted ribbons[45] that were assumed to be helical aggregates of amphiphilic molecules;[37] optical micrographs support a single twisted crystalline ribbon. Cholesteric liquid-crystal twisting is not discussed herein as the infinitesimal twists between layers of molecules are not consistent with a typical space groups.[46] However, liquid-crystal molecules can also form heterogeneous media with embedded twisted morphologies, as in the helical nanofilamentous B4

Alexander G. Shtukenberg was born in Leningrad in 1971. He got a specialist degree in 1993 at Geological Faculty of Saint-Petersburg State University, Russia. Under the supervision of Yuri Punin, he received a Candidate of Science degree in 1997 and continued to work at Geological Faculty as a researcher and faculty member. In 2009 he earned the Doctor of Science degree and in 2010 became a professor at the same university. Since 2010 he has been working with Bart Kahr at New York University.

Bart Kahr was born in New York City in 1961. He studied chemistry with I. D. Reingold at Middlebury College, with Kurt Mislow at Princeton University (PhD, 1988), and with J. M. McBride at Yale University. He was a faculty member at Purdue University from 1990–1996 and at the University of Washington, Seattle from 1997–2009. Currently he is professor of chemistry in the Molecular Design Institute at New York University. His research group studies the growth, structure, and optical properties of single crystals and polycrystalline patterns.

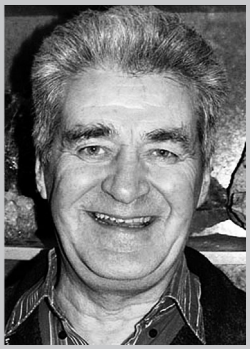

Yurii O. Punin was born in Leningrad (now Saint-Petersburg, Russia) in 1941. He got a specialist degree (1963) and a Candidate of Science degree (equivalent of PhD, 1970) at Geological Faculty of Leningrad State University and worked there as a researcher. He defended the Doctor of Science degree (equivalent of habilitation) in 1994, the next year was appointed professor of crystallography/mineralogy at the Crystallography Department of the same university.

Ankit Gujral earned his bachelor's degree in chemistry at New York University under the guidance of Professor Bart Kahr. He is currently a graduate student at the University of Wisconsin-Madison working in the group of Professor Mark Ediger.

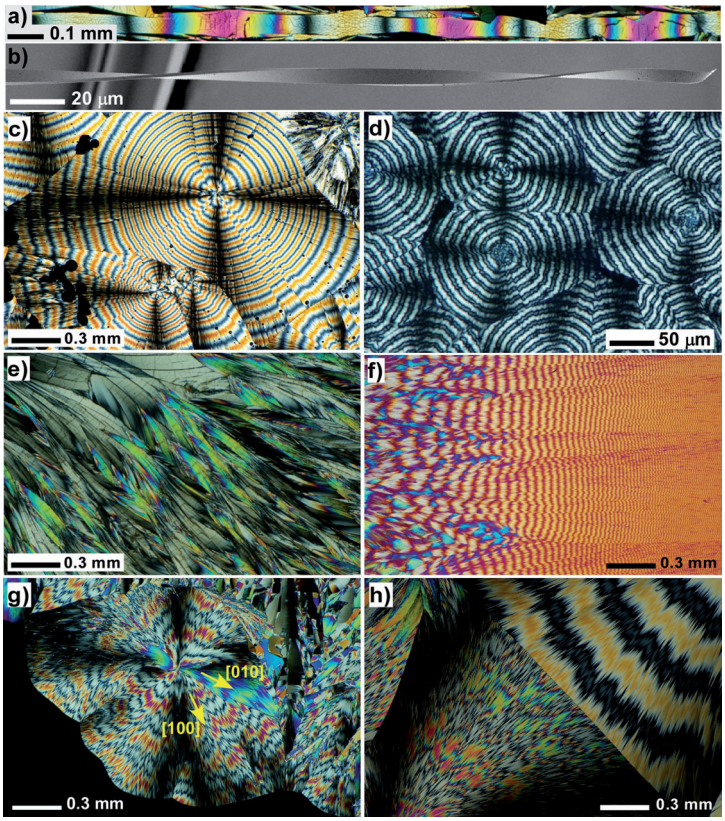

Figure 1. a) Ribbon of hippuric acid grown from the melt viewed between crossed polarizers. Progression of black bands with alternating large and small spacing correspond to angular distances between optic axis outcrops as the crystal rotates around the [100] axis. b) SEM image of twisted hippuric acid ribbon grown by sublimation.[9] The twisting that is implied in (a) by the progression of interference colors is now evident. c) Aspirin with admixture of Canada balsam, approximately 15 wt.%. Spherulite cores grew at 4 °C whereas the outer parts grew at 20 °C; d) Poly(3-hydroxybutyrate) spherulites with a constant band spacing; e) Hippuric acid. Irregular arrangement of bunches of [100] elongated twisted fibers is expected to be due to the growth rate anisotropy in the (100) plane; f) Tetraphenyl lead with admixture of polyvinylpyrrolidone (PVP), 24.5 wt.%. The band spacing decreases from 160 to 8 μm, as the growth temperature decreases. First order red wave plate is inserted between crossed polarizers. Predominantly [100] fibers are shown, whereas the blue interference colors correspond to domains with untwisted [001] fibers;[6] g) Testosterone propionate banded spherulite (stable polymorph) with fibers twisted around [100] throughout most of the spherulite.[10] A small area with alternating blue and green interference colors corresponds to [010] fibers; h) Banded spherulites of β resorcinol (lower left) and undefined resorcinol polymorph (upper right) between crossed polarizers. Crystals grown from the melt at 50 °C in the presence of L-tartaric acid. Reproduced from Ref. [11] with permission.

phase,[47–51] that should not be wholly overlooked in the context of this Review.[52–55]

And what of bending? Does scrolled graphene belong here? Scrolled graphene, flattened, would be defined by only two basis vectors. Single-atom-thick layers do not a crystal make. How many graphene strata of a multi-layered scroll are necessary before we begin to speak of bent graphite?[56] It is hard to say. No classification scheme is perfect. Our set of twisted crystals will surely not be the same as someone else's. But, by laying-out criteria clearly, illustrating them richly, and breaking them when convenient for good reason, we can lessen confusion that might be engendered by our set.

Table 1 summarizes crystals ranging from the nanoscopic to macroscopic (cm) that twist and bend as a result of intrinsic growth phenomena.

2. History

The earliest description of a twisted crystal of which we are aware of is phosgenite ($Pb_2CO_3Cl_2$) reportedly found in Sowerby's *British Mineralogy* (1811)[57] by Spencer (Figure 5a).[19] Other twisted minerals described in the 19th Century include stibnite (Sb_2S_3;[58] Figure 5b) from Wada's *Minerals of Japan* (1904).[59] But how these specimens got this way is not surely known.

Lehmann, a pioneer in the development of the hot-stage microscope, was the first to focus on laboratory-grown twisted crystals.[60] He observed a variety of substances with twisted habits some of which are rendered in Figure 6. Lehmann reported that twisted crystals, on thickening, would untwist, often so violently that they shattered into pieces.

The biologist Haeckel was enthusiastic about the work of Lehmann, particularly the latter's investigations of liquid crystals. Haeckel[61] studied the self-patterning of small-molecule banded spherulites, likely obtained from Lehmann, because he believed that these self-organizing polycrystalline systems were "missing links" between animate and inanimate matter.[62] We now know that many banded spherulites of the type studied by Haeckel and especially by Bernauer comprise twisted fibrils.

A naturally occurring, banded spherulite of chalcedony, the fibrous form of quartz, was described by Michel-Lévy and Munier-Chalmas[63] and others later.[64–69] They were predisposed, presumably by Lehmann, to interpret the alternating light and dark bands between crossed polarizers as a consequence of the helical precession of the optic axis. Lacroix observed something similar in phosphorites.[70] But, minerals offer little opportunity to observe and modulate growth.

Wallerant, a pioneering liquid-crystal researcher, also studied fibrous quartz[71] and was likely sensitized to twisted crystals in this way. He intended to mimic the twisting of quartz with materials in the laboratory. At the turn of the 20th Century, the expression of molecular dissymmetry in crystal form, as in Pasteur's tartrate hemihedra,[72] was by no means predictable (it still isn't). Helical crystals in thin films gave optical signatures in polarized light that made dissymmetry vivid. Among Wallerant's chalcedony mimics were resorcinol, hydroquinone, glycolic acid, and malonamide.[73–75] In fact, in 1906, Wallerant reported that these substances crystallize from the melt as mesoscale helical fibers, twisting right or left depending on the configuration of chiral additives, such as tartaric acid.[74] By noting the changes in band positions while rotating a crystal about a radius or fiber axis, Wallerant was able to assign the sense of his crystalline helices just as the sense of

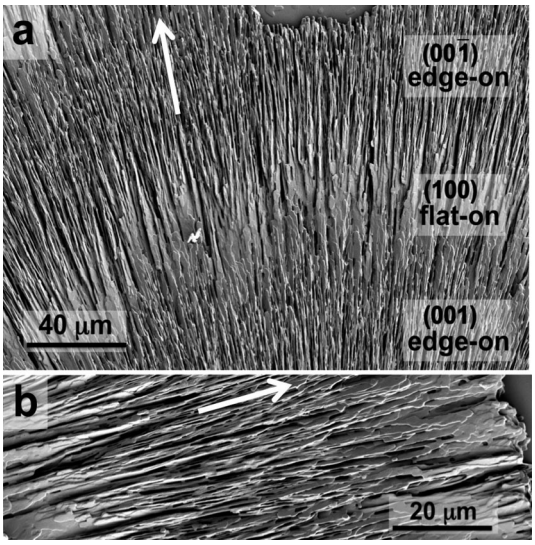

Figure 2. a) Scanning electron micrograph of banded aspirin spherulite showing, from bottom to top, edge-on half band of crystallites transforming into flat-on half band, and then to edge-on again. b) Scanning electron micrograph emphasizing twisting of lamellae. White arrows marks growth directions. Reproduced from Ref. [13] with permission.

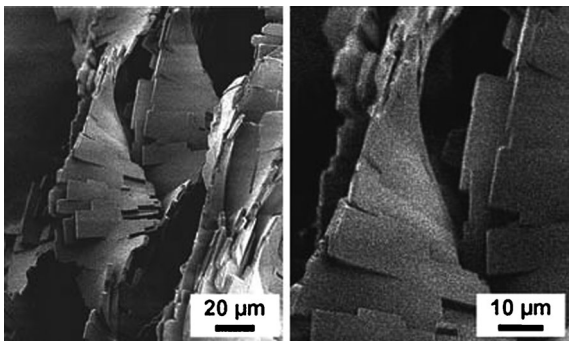

Figure 3. Helical twisting of potassium dichromate grown from gel. Reproduced from Ref. [32] with permission.

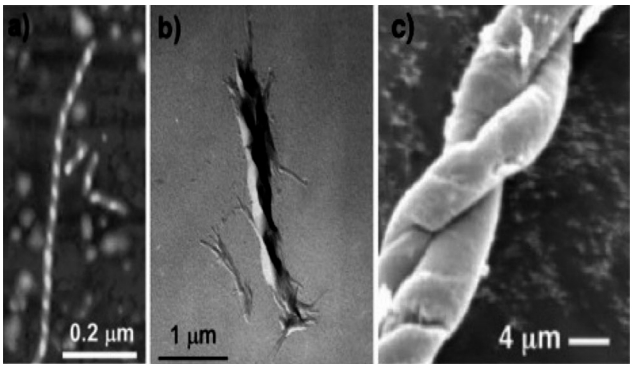

Figure 4. Twisted crystals? a) Tau fibril. Reproduced from Ref. [40] with permission. b) Silk fibroin. Reproduced from Ref. [41] with permission. c) Polyphenylacetylene with cyclodextrin pendants. Reproduced from Ref. [43] with permission.

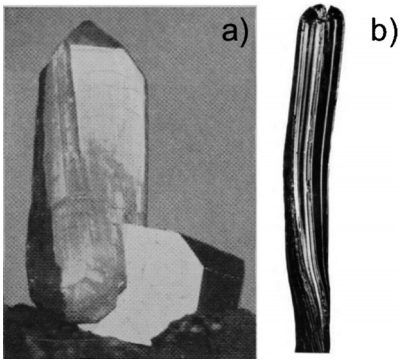

Figure 5. a) Phosgenite, $(PbCl)_2CO_3$, from Derbyshire. Prismatic crystal with helical twist around the vertical axis growing in concert with untwisted crystal at the base. British Museum specimen no. 59296. These crystals were shown in J. Sowerby, *British Mineralogy* (London, **1811**, *vol. 4*, p. 175, plate 399) according to Spencer.[19] b) Stibnite (Sb_2S_3).[59]

Table 1: Overview of twisted crystals and related objects.

Object	h[a]	$2P$ or R[b]	γ[c]	Growth medium	Stress relaxation[d]
Molecular and ionic spherulites	0.02–1 μm	1–10 μm	0.0003–0.003	Melt, seldom solution	Point defects, dislocation ensembles; $\xi \approx 1$
High polymer spherulites	5–20 nm	0.5–3 μm	0.0005–0.01	Melt, seldom solution	Molecular conformations, dislocations
Nanoscale single crystals	10–500 nm	0.3–10 μm	0.002–0.04 up to 0.4	Vapor phase, sometimes solution and flux	Dislocations, point defects; $\xi = 0$–1
Meso- and macroscale single crystals	0.3 μm–5 cm	0.2–100 mm	0.001–0.4	Solution, gel, sometimes melt and vapor phase	Dislocation ensembles; $\xi \approx 1$
Polycrystalline and amorphous aggregates of unusual curved morphologies	20 nm–20 μm	0.1–100 μm	No curvature related stress	Solution, gel, vapor phase	No curvature related stress
Transrotational crystals	5–80 nm	10–200 μm[e]	0.003–0.01	Amorphous film	Dislocations, point defects; $\xi = 0$–1
Aggregates of amphiphilic molecules and liquid crystals	10 nm–5 μm	20 nm–10 μm	0.01–1	Solution, liquid crystals	Molecular conformations
Nano-objects with 2D translational periodicity; nanotubes, nanoscrolls	0.5–10 nm	8–80 nm	0.01–0.1	Solution, vapor phase	Molecular conformations, point defects

[a] Smallest dimension. [b] Minimum twist period, $2P$ (2π rotation) or radius of curvature, R. [c] Maximum strain, $\gamma = \pi h/P = h/(2R)$. [d] Type of predominating elastic stress relaxation; ξ is a fraction of relaxed elastic stress. [e] Internal curvature of the lattice recalculated as pitch for comparison.

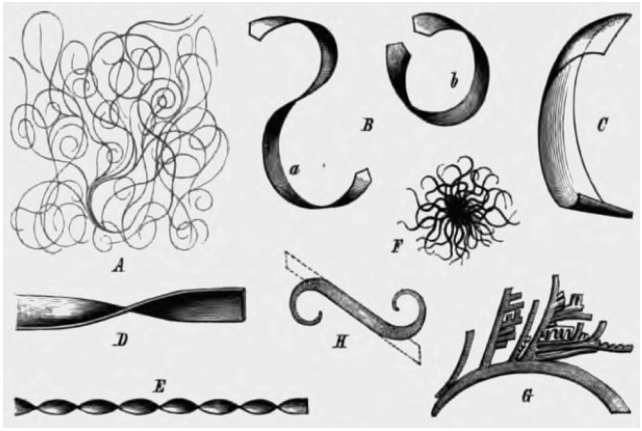

Figure 6. Bent, scrolled, and twisted crystals from Lehmann.[60] A) $CrCl_2 + HgCl_2$ solid solution, B) chiral 1,2-diphenylethane-1,2-diyldiacetate (stereochemistry unknown), C) (*Z*)-cinnamic acid, D) $K_2Cr_2O_7$, E) hydroxyquinoline, F) 4-methyl-2,6-dinitrophenol + aniline cocrystal, G) 2,5-dihydroxy-3,6-dipropionylcyclohexa-2,5-diene-1,4-dione.

a screw's threads can be gauged by rotating about its long axis. He was impressed by the smooth progression of the optical properties and argued that their character was inconsistent with helical arrays of untwisted crystals.

Pure resorcinol crystallizes from the melt as spherulites without optical modulation. Wallerant shrewdly recognized that twisting and optical banding were intimately associated with optical activity. In other words, he was able to directly correlate small-molecule configuration and mesoscale helix sense. Wallerant found two spherulitic polymorphs of greater and lesser linear birefringence on crystallization from the melt. We showed that the β form[76] and a new polymorph (Figure 1h), twist stereospecifically under the influence of tartaric acid.[11]

Wallerant's studies of so-called "helicoidal" crystals were enriched by Gaubert who described in 1908 banded spherulites of cholesterol,[77] several opiates,[78,79] and elemental sulfur.[80] Gaubert papers on twisted crystals spanned the period from 1908–1931.[81–90] Both Wallerant and Gaubert strongly influenced Bernauer. Unfortunately, their collective line of research did not survive Bernauer's death. He was killed by a bomb in Berlin in the Spring of 1945. Systematic studies of twisted and bent small-molecule and ionic crystals abruptly ceased. The occasional serendipitous discovery of a twisted crystal was generally treated as a curiosity, wholly divorced from earlier history. One exception was Shubnikov who was fascinated by crystalline ensembles of symmetry ∞/∞, likewise the symmetry of an optically active solution. Spheres of thin, compact twisted radii conform to this point symmetry as determined by visible light. Shubnikov, in his classic book on symmetry with Kopstik,[91] illustrated malonamide and triphenylmethane ring-banded spherulites, although the latter seem to arise from rhythmic crystallization rather than helical twisting.[92]

The synthetic polymer industry emerged after World War II. Not long thereafter, banded spherulites of high-polymers were discovered and their study has dominated the discussions of crystal twisting ever since. The main feature of ring-banded polymer spherulites, the smooth rotation of the optical indicatrix along radii, was established by Point,[93,94] Keith and Padden,[95,96] Keller,[97] and Price.[98] There have since been several hundred publications on the origins of helical twisting in high-polymer spherulites (Section 5.6). These were reviewed by Lotz and Cheng[99] who concluded that understanding the origins of "*twisting remains one of the major challenges in the research field of polymer morphology. It apparently has not been settled…*". Herein, by embracing all classes of materials, new mechanisms might come into focus that may also clarify questions within the domain of polymers. This sentiment was expressed by Keller in *Nature* in 1952,[100] but the problem has not heretofore been tackled in its totality.

3. Overview of Bent and Twisted Crystals

Twisted crystals form most commonly as fibrils in melt-grown spherulites of small-molecule organic compounds and high polymers. The 135 examples of small-molecule banded spherulites with twisted fibers listed in *"Gedrillte" Kristalle*[1] is the greatest collection of such forms. Many of these compounds are distinguished by their simplicity and commonality including: urea, phenol, quinone, chlorobenzene, malonic acid, aspirin, and catechol. Most of Bernauer's substances, 95% or so, have never been studied since. Hippuric acid (Figure 1a,b) is an exception.[6–8,101] Kuhnert-Brandstätter et al. found a number of twisted steroids.[389] Additional examples of banded organic spherulites can apparently be found in the *Latvian Pharmaceutical Journal* (1934).[102]

Newly discovered banded spherulites of small organic compounds are reported, occasionally. These include testosterone propionate,[10] tetraphenyl tin,[6] mannitol in both its α and δ phases (Figure 7),[103–105] 4-cyano-4′-decyloxybiphenyl,[106–108] and hexa-*peri*-hexabenzocornene.[109] Natural fibrous quartz, chalcedony, is the most common inorganic compound that forms banded spherulites.[63–69] Rare spherulite-forming minerals with twisted fibers include prehnite ($Ca_2Al(AlSi_3O_{10})(OH)_2$).[110] Even elements, C (graph-

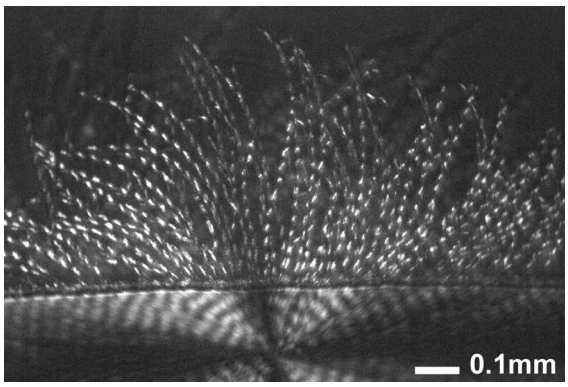

Figure 7. A compact banded δ-mannitol spherulite growing from the melt (bottom third of image) turns into an open spherulite with isolated twisted fibers when it penetrates a vapor bubble. Reproduced from Ref. [105] with permission.

ite),[111–114] S,[115] and Se,[116,117] have been shown to form ring-banded spherulites composed of twisted needles.

Banded spherulites are formed in naturally occurring high polymers such as the latex of gutta-percha[118] as well as monodispersed long-chain paraffins ($C_{294}H_{590}$).[119] Polyethylene spherulites have been studied more intensively than any other family of polymers in this regard.[95,96,120–133] Polyesters[95,135–147] such as poly(3-hydroxybutyrate)[148–155] and polyamides,[156,157] frequently form spherulites composed of twisted fibrils. In some cases, the sense of twisting could be correlated with the configuration of monomers as in poly(D- or L-lactic acid).[134,158–160] Twisting also has been studied in poly(epichlorohydrin),[161–163] poly(vinylidene fluoride)[164–167] and isotactic poly(1-butene),[168] among other substances, including block copolymers.[169]

Twisted and bent single crystals—not packed in spherulitic mats—come in all sizes from the nanoscopic and mesoscopic, to the macroscopic. This size classification is based on the cross-sectional dimension. Although there is no fundamental disjunction with scale, twisting forces and stress relaxation processes may be different as discussed in Section 5.

Among nanoscopic twisting crystallites (thickness h between 5 and 500 nm) we find lamellae of high polymers,[170–173] as well as proteins, such as deoxyhemoglobin S,[174] and a variety simple polypeptides, such as (D- and L-Ala-Gly)$_n$.[41] Branched alkanes can form scrolled nanolamellae[175] whereas salts of 12-hydroxysterate sometimes precipitate twisted nanoribbons.[176,177] A variety of twisted nanowires and rods grow from the vapor, including PbS,[178] PbSe,[179] and β-SiC.[180] Even simple cubic alkali halide salts can be made to grow with very anisotropic and twisted habits from aqueous solution.[181–183] Yang and Kotov have recently reviewed twisted inorganic nanostructures.[184] In particularly, such structures include nanorings and nanohelices of ZnO (Figure 8), GaN, AlN, InP, $Ag_2V_4O_{11}$, and SnO_2.[185–197]

Mesoscopic twisted crystals (ca. 500 nm $< h <$ 100 μm) include 10,12-tricosadynoic anhydride[45] and (1,4-bis[2-(pyrene-1-yl)vinyl]-2,5-dimethylbenzene)IBr_2.[198] The chiral, polycyclic aromatic hydrocarbon decacyclene forms left- and right-handed twisted mesoscale ribbons.[199] 2,5-Di-*tert*-butyl-1,4-dimethoxybenzene plates curl as they precipitate from solution.[200] Mannitol,[105] hippuric acid,[7,8] and resorcinol[201] can all be made to grow in this size regime as single twisted needles as well as banded spherulites. $K_2Cr_2O_7$,[6,202–205] (Figure 3), H_3BO_3,[32,202–204] and aspartic acid[31] crystallize from gel as mesoscale twisted ribbons that organize into spherulites. Sn[206] and Pd[207,208] are elements that form twisted whiskers, a morphology that is also expressed by sapphire (α-Al_2O_3)[209,210] and ZnS.[211] The following binary alloys grow as twisted lamellae on the mesoscale: Pb-Sn, Al-$AgAl_2$, Al-$CuAl_2$, Al-Zn.[212–214] ZrS_2 forms scrolls.[215,216] Natural rutile (TiO_2), cosalite ($Pb_2Bi_2S_5$), stibnite (Sb_2S_3), and chalcotrichite (Cu_2O) form twisted fibrous crystals.[217] Magnesium-rich calcite does likewise.[218]

Quartz[219–225] (Figure 9a) joins Sowerby's[57] phosgenite and Wada's stibnite (Figure 5) as a twisted macrocrystal (100 μm $< h <$ 3 cm). Examples were illustrated in the *Mineral Kingdom* by Brauns and others subsequently.[226,227]

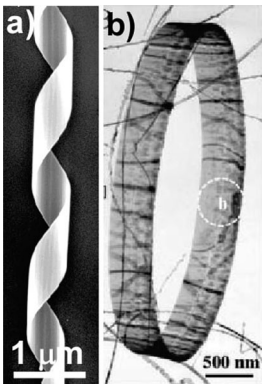

Figure 8. a) SEM image of twisted ZnO nanoribbon. Reproduced from Ref. [189] with permission; b) Bright-field TEM of dislocation free, single-crystalline ZnO nanoring. Reproduced from Ref. [187] with permission.

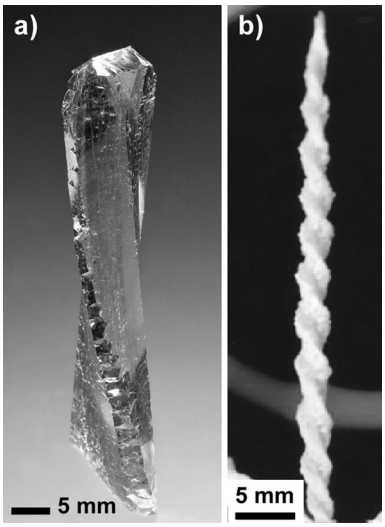

Figure 9. Twisted macrocrystals. a) Natural quartz. Reproduced from Ref. [256] with permission; b) $K_2Cr_2O_7$. Reproduced from Ref. [252] with permission.

Quartz can be twisted along [0001] or $[11\bar{2}0]$. Micas exhibit complex distortions as they bend about more than one axis.[228–230] Cubic pyrite is simultaneously twisted about all four ⟨111⟩ directions[221,231,232] as shown in Figure 10b. Large saddle-shaped dolomites have been described by Miers (Figure 10a),[233] among others.[234–238] Jamesonite ($Pb_4FeSb_6S_{14}$) forms elongated crystals bent normal to the direction of extension.[217] Macroscopic bent minerals include orpiment (As_2S_3),[239] spiral apatite ($Ca_5(PO_4)_3F$),[240] scrolls of molybdenite (MoS_2),[241] millerite (NiS),[242] corundum (Al_2O_3),[243] fluorite (CaF_2),[243] augite (Ca(Mg,Fe,Al)-[(Si,Al)$_2O_6$]),[243] among some others. Monoclinic gypsum, elongated along [001] and bent around [010] can be found in nature[19,217] but it can also be prepared in the laboratory.[244–247] $K_2Cr_2O_7$ forms very large helices, pictured in Figure 9b when grown from aqueous gels.[248–252] Twisted oxalic acid dihydrate precipitates from several organic solvents.[253–255]

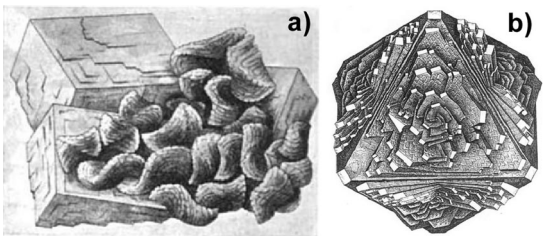

Figure 10. a) Saddles of dolomite on fluorite cubes.[233] b) Pyrite (4 mm in size) twisted about four threefold axes. Reproduced from Ref. [232] with permission.

4. Phenomenology

4.1. Morphology of individuals

What precisely are the shapes of twisted crystals? How best to define their strange habits? Twisting and/or bending around some direction produces curved forms. Locally, deformation of the crystal lattice can be described by a second-rank tensor of curvature with principal values κ_1, κ_2, and κ_3.

Ribbon-like crystals (length (L) $\gg$ width (H) $>$ thickness (h)) generally bend around two mutually perpendicular axes in the ribbon plane. They are characterized by the two constant principal surface curvatures κ_1 and κ_2, and an angle ϕ in the ribbon plane between the ribbon elongation direction and one of the bending axes (Figure 11).[257] In the general case, the ribbon will form a helix where the central line wraps around a bounding cylinder whose radius is calculated directly from the aforementioned parameters.[257]

Pure twist deformations (helicoids) of many needle- and ribbon-like single crystals and crystallites bound within spherulites (Figure 1 c,d, Figure 2, Figure 7) are described by $\kappa_1 = -\kappa_2$, $\phi = \pm\pi/4$. The spine of the ribbon and cross sections remain straight. Twisting is characterized by a pitch, $P = \pi/\theta$, the length required to achieve a 180° rotation, where θ is the twist per unit length. The curvature and the pitch are related by $\kappa_{1,2} = \pm P/(r^2+P^2)$, where r is the distance from the spine in the plane of ribbon.

A ribbon forms a ring with positive Gaussian curvature if either $\kappa_1 = \kappa_2$, $\phi = 0$, or $\phi = \pi/2$. If either κ_1 or $\kappa_2 = 0$, the ribbon bends into a cylinder with zero Gaussian curvature ($\kappa_1 + \kappa_2 = 0$). For example, bending around the short axis can result in cylindrical rings and helices, which are common for ZnO, GaN, and AlN nanocrystals (Figure 8). Scrolls of plate-like crystals ($L \approx H \gg h$) have been observed for graphite,[111–114] molybdenite,[241] and γ-poly(vinylidene fluoride).[167] The curvature or radius of curvature, $R = 1/\kappa$, gives the magnitude of the deformation.

The range of morphologies that can be expressed in the mutual orientation of bending axes with respect to the crystal extension was captured in a clever mathematical experiment.[257] Chen et al. stretched a square piece of latex twice as much in the vertical direction as in the horizontal direction. An adhesive sheet was attached to the strained latex and subsequently cut into ribbons with long axes varying between 0° and 90° in 15° intervals. On release, the strips bend about orthogonal axes at the extremities and twist into helical forms at intermediate angles (Figure 11). A helicoid, a common form not captured in Figure 11, would be a consequence of equal twists about the axes 45° and −45° with respect to the long axis, is shown at right in Figure 12.

While bent crystals and twisted crystals form by similar mechanisms, twisting is much more common. This is because twisting about the growth direction does not interfere with forward propagation, and is consistent with linear gradients in media that commonly drive growth. Such objects can twist by any n-multiple of π with constant pitch producing eye-catching periodic structures. Bending around an axis perpendicular to the growth direction may interfere with growth after a bend of 2π while the tip returns to a region of space that may no longer support growth.

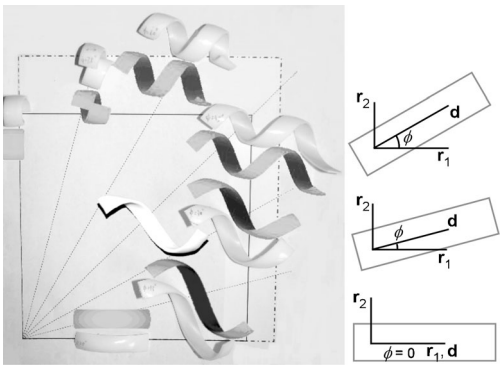

Figure 11. A square piece of latex was stretched twice as much in the vertical direction than in the horizontal (dashed-dotted edges). An adhesive sheet was bonded to the strained latex and subsequently cut into ribbons with long axes varying between 0° and 90° in 15° intervals. After release, the forms were displayed on the appropriate stretching coordinate along with the theoretical prediction. Directions $\mathbf{r}_1$ and $\mathbf{r}_2$ correspond to the principle bending directions characterized by the curvatures κ_1 and κ_2, respectively. $\mathbf{d}$ = direction of the ribbon elongation. Reproduced from Ref. [257] with permission.

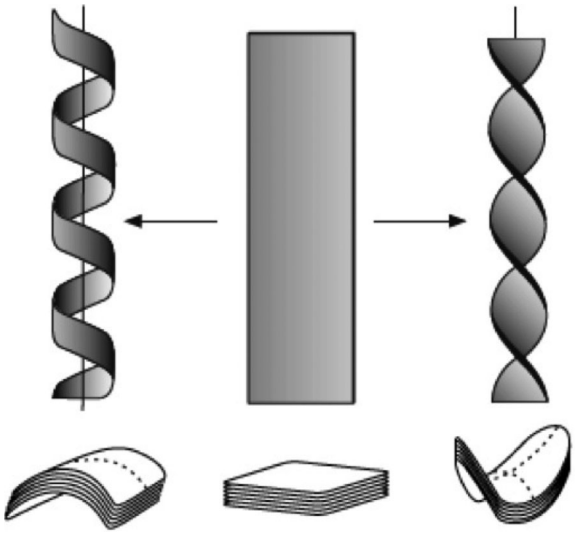

Figure 12. Distortion of a plank with zero curvature (center) to give a cylindrical helix with positive curvature (left) or a helicoid with negative curvature (right). Reproduced from Ref. [258] with permission.

Pure twist of vanishing thickness—all surface—is a helicoid that gives a line in cross section. Real "helicoids" of finite thickness, such as macroscopic quartz crystals, often show S-shaped cross sections.[219,254] Not surprisingly, enantiomers of poly(L-lactic acid) and poly(D-lactic acid) lamellae show enantiomorphous "S" shapes.[134,160] But, for large, cylindrical or even isometric crystals ($L \gg H \approx h$ and $L \approx H \approx h$, respectively), the scheme of deformation can be very complex because twisting and bending of similar strengths around several directions are possible. As a result, deformation may become inhomogeneous with local curvatures varying from point to point producing vexing morphologies.

Deformation can be inhomogeneous even for ribbon-like crystals. Twisting around the longest axis may be complicated by twisting around a perpendicular axis. The spectacular dark-field transmission electron micrographs (TEMs) by Cheng and co-workers revealed that there is a helical twist not only along the axis of the ribbon, but also perpendicular to it; bright arcs from selected reflections do not illuminate the whole ribbon in cross section (Figure 13).[172,259] Interpreting morphology from cross sections of twisted objects at the interfaces of spherulites by microstructural techniques, such as atomic force microscopy (AFM) or SEM is challenging.[99,143,152,260]

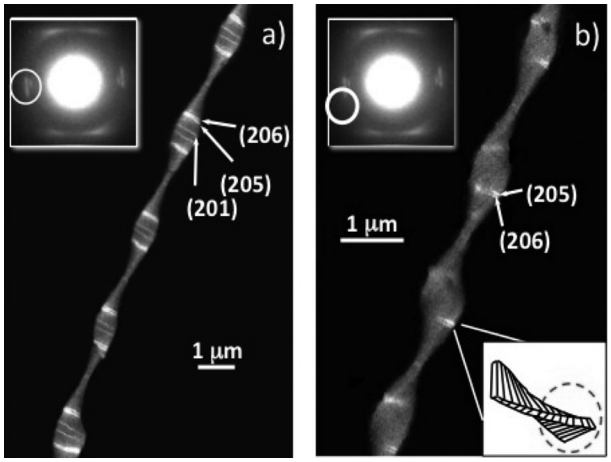

Figure 13. a) Dark field TEM of doubly twisted helical lamellar crystal of (*R*)-(−)-4′-{ω-[2-(*p*-hydroxy-*o*-nitrophenyloxy)-1-propyloxy]-1-nonyloxy}-4-biphenylcarboxylic acid constructed from complete diffraction arcs. b) Same as (a) but from partial diffraction arcs showing the partial illumination of cross sections that indicate the double twist. Reproduced from Ref. [259] with permission.

For elongated crystallites (needles, fibers, ribbons) of constant cross-sections grown under constant conditions, pitch is constant along the fiber. This is true from the nano- to the macroscale (Figure 8a, 9). Oxalic acid dihydrate forms $(\bar{1}01)$ plates or [010] elongated crystals twisted around [010] and forming complex saddle-like shapes when grown from acetone, acetic acid, formic acid, butanol, or succinic acid (Figure 14).[253–255] If twisting is slight (Figure 14a) the crystals are homogeneously distorted as confirmed by detailed goniometric study (Figure 15). In contrast, twisting is not homogeneous over the quartz crystal (Figure 16). Sometimes

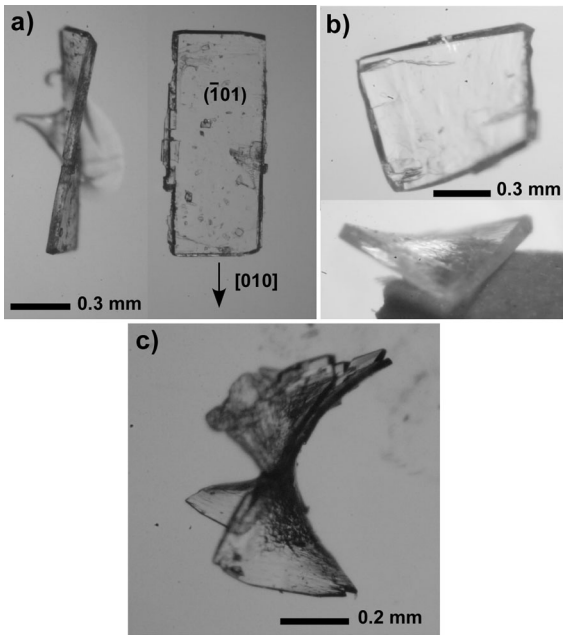

Figure 14. Oxalic acid dihydrate crystals from acetic acid.[255] a) Elongated crystal with large pitch in two different orientations. b) Squarish plate-like crystal with intermediate twist intensity in two different orientations. c) Strongly twisted crystal with macroblock splitting.

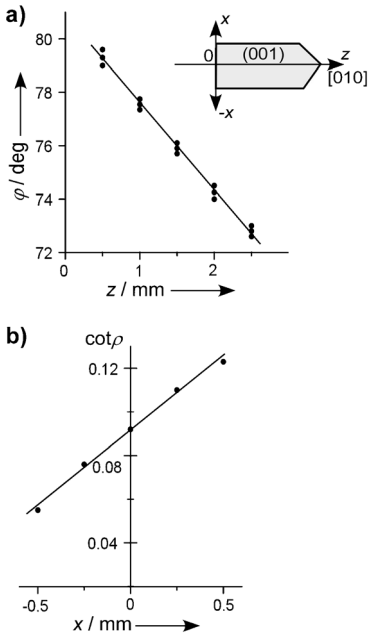

Figure 15. Spherical coordinates, ϕ and ρ, measured with a Goldschmidt light goniometer for the (001) face of twisted oxalic acid dihydrate crystal grown from acetone.[219,253] a) Three profiles measured across the crystal, $x = 0$. b) A profile measured along the central line, z = constant. Inset: the coordinate system and orientation of the twisting axis [010]. Straight fits indicate constant pitch and constant twist intensity in the cross sections.

ribbon-like crystallites twist unevenly—relatively long straight regions alternate with abrupt changes of crystallite orientation, as observed for individual fibers of deoxyhemo-

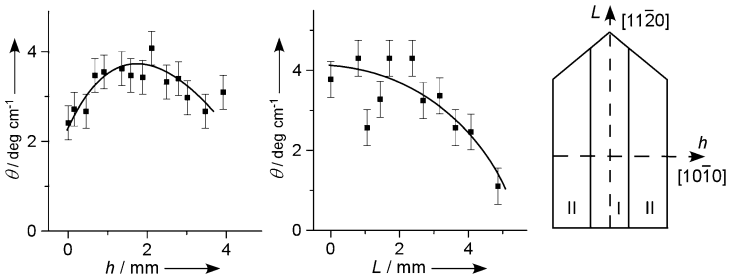

Figure 16. Inhomogeneity in the distribution of the twist intensity θ, measured along two profiles of the same natural quartz crystal.[219] Regions I and II correspond to two stages of quartz growth: along [11$\bar{2}$0] without and with thickening, respectively. Pitch measured as the angular deviation of the optic axis outcrop from the normal to the crystal cut.

globin S[174] and mannitol[105] as well as polymer lameallae in spherulites[140,167] and millerite whiskers.[217] This may be a consequence of mechanical interactions between growing crystallites and the substrate or mutual crystal crowding. If growth conditions and/or cross section dimensions vary, pitch will likewise vary (Figure 1 f).[144]

Deformations along symmetry related directions should be comparable (e.g. the four threefold axes of pyrite[221,231] and the three $\langle 11\bar{2}0\rangle$ directions of dolomite;[1,233] Figure 10). Symmetry independent directions can be different (e.g. threefold and twofold axes of quartz,[219,220,222] the [100] and [010] directions of mica[219,228]). Quartz will elongate along, and twist about, the two- or threefold axis.[219,225] We have observed that testosterone propionate can be twisted (with different pitches) about all three independent crystallographic axes (Figure 1 g).[10]

4.2. Morphology of Aggregates

Banded spherulites are typically composed of numerous fine fibers radiating from a common center and show concentric rings of optical contrast between crossed polarizers (Figure 1). Since the orientation of the optical indicatrix is fixed with respect to the crystal structure, optically anisotropic twisted fibers show a periodic change of retardance, the phase difference between the orthogonal rays propagating within the sample, with a period equal to a π rotation.

Banding in spherulites may arise not only from fiber twisting but also from rhythmic precipitation.[6,99,137,141,163,261–265] The origin of banding can be resolved by the direct detection of twisted forms by microstructural methods of analysis, such as AFM or SEM (Figure 2). If direct observations are not possible, fiber twisting can be established by Wallerant's method of "sensing the screw".[6,8,95,160,161,266,267] Upon tilting a fiber clockwise (defined while viewing from the advancing interface toward the nucleus) the extinction bands observed between crossed polarizers shift further or nearer to the observer depending on whether the helix is right or left handed, respectively (Figure 17).

We have illustrated the optical sensing of the screw quantitatively with Mueller matrix microscopy.[8] Generally speaking, banded spherulites have been a rich source of phenomenology for optical crystallographers. Keller simulated micrographs in polarized light as a function of the angle of the fibrous twisting crystals to the substrate.[97,150] Linear birefringence imaging of banded spherulites using quantitative light-intensity measurements were introduced by Ye et al. Figure 18 a,b[267] was obtained with the PolScope.[268] Further, studies of circular birefringence by Mueller matrix imaging have been instructive in unraveling the mesoscale stereochemistry associated with multilamellar, linearly birefringent layers.[8,105] For instance, in this way, we can distinguish enantiomorphous halves of twisted aspirin spherulites as shown in Figure 18 d.[13,269]

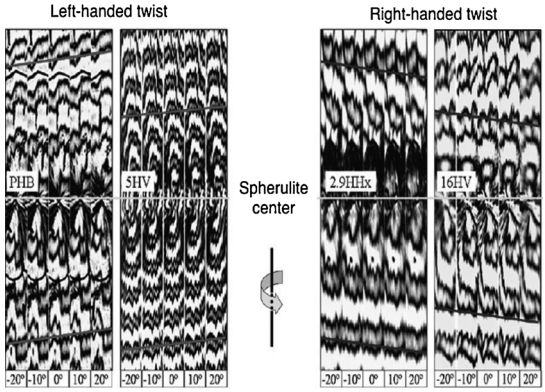

Figure 17. Sensing the screw. Motion of extinction bands in polymer spherulites upon rotating the sample about the radius in direction indicted by arrow. PHB = Poly(*R*-3-hydroxybutyrate), 5HV and 16HV = polyhydroxybutyrate copolymer with 5% and 16% hydroxyvalerate monomers, respectively, 2.9HHx = polyhydroxybutyrate copolymer with 2.9% hydroxyhexanoate monomers. Reproduced from Ref. [152] with permission.

Today, microfocus X-ray diffraction,[6,154] as shown in Figure 19,[153] microbeam small- and wide-angle X-ray scattering,[144,145] and polarized micro-Raman spectroscopy can likewise be used to establish the sense of twist.[146]

One barely characterized optical characteristic of non-absorbing fibrous spherulites is their scattering of linearly polarized light. This phenomenon was called *pseudopolychroism* or *pseudopleochroism* by Gaubert[81,89] and Bernauer,[1,270] and manifests itself as linear extinction in contemporary polarization modulation imaging. The importance of light scattering in interpreting the optical properties of tightly ring-banded spherulites was recently emphasized by Point.[271] The optical transform method was used by Morgan to interpret the X-ray scattering patterns of ring-banded spherulites.[272,273]

Ideally, all fibers twist in-phase forming a cooperative banded pattern, but this only occurs if fiber cross-sections are isometric and the only type of deformation is axial twisting. In reality, most spherulite fibers are ribbon-like or lamellar and pure axial twist is impeded by collisions among lamellae and the necessity of cooperative distortions.[129] The lamellae can deviate from radial directions, stick to each other, re-nucleate, and form chaotic patterns (Figure 1 e). This sometimes results

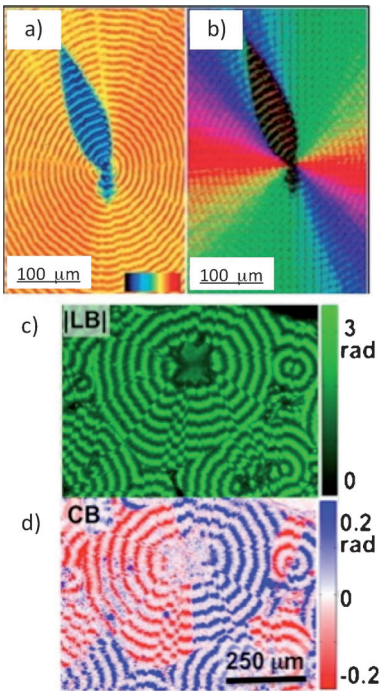

Figure 18. a,b) Polyhydroxyvalerate. a) False color map of linear retardance $|\sin(\delta)|$ (color scale from 0 to 1) and b) linear extinction at $\lambda = 546$ nm. Color scale from 0° to 180° measured counterclockwise from the horizontal. Reproduced from Ref. [267] with permission. Azimuths mark direction of slow axis. "Eye" and surrounding region have different twist senses. c) Linear retardance ($|LB|$) and d) circular retardance (CB) micrographs ($\lambda = 532$ nm) of aspirin spherulites. Reproduced from Ref. [13] with permission.

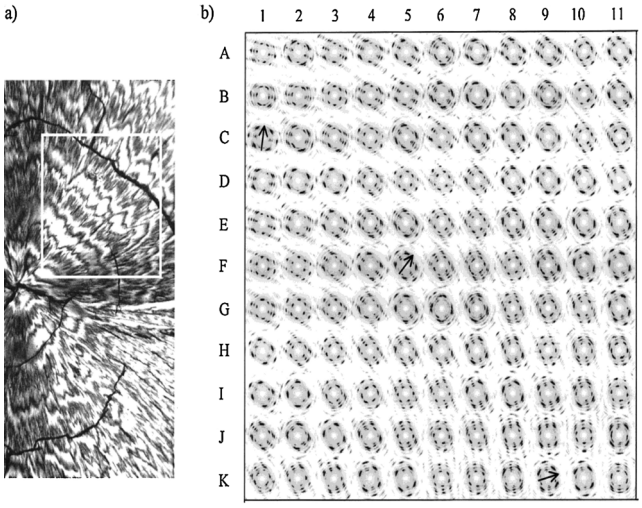

Figure 19. a) Poly(*R*-3-hydroxybutyrate) spherulite between crossed polarizers. The white square marks the area investigated by microfocus X-ray diffraction, 300 μm × 300 μm. b) Local Laue patterns. The arrows indicate the radial *a* axis. Reproduced from Ref. [153] with permission.

in the formation of domains within the same spehrulite with different directions of growth and different twisting axes (hippuric acid,[6] tetraphenyl lead (Figure 1 f),[6] testosterone propionate (Figure 1 g),[10] poly(3-hydroxyvalerate) (Figure 18 a,b)[267]).

Just as inhomogeneities occur in the twisting of individual crystallites (Section 4.1), spatial and temporal inhomogeneities are also evident in aggregates of fibers in banded spherulites which gives rise to very complicated optical textures.[99,165,167,267,274–276] In general, a theory of the organization of twisted lamellae in spherulites is still lacking. It is well established from observations of poly(L-lactic acid),[120] poly(ethylene),[124,125] poly(*R*-3-hydroxybutyrate),[148] poly(vinylidene fluoride),[166] as well as our observations on mannitol and tetraphenyl lead (Figure 1 f) that well-organized banded patterns arise only if the twist period is small. Intense twisting seems to suppress all other inhomogeneities.

4.3. Correlations of Molecular and Mesoscale Chirality

Helices and helicoids are chiral and researchers naturally have tried, mostly in vain, to establish correlations between macroscopic chiral morphologies, and molecular configuration or crystallographic symmetry. Researchers speak of "levels of chirality".[277] The primary molecular level of chirality presumably propagates to the secondary level, the handedness of helical macromolecules, for example. These confirmations may further establish enantiomorphous macro- or mesoscopic morphologies with opposite twists, the tertiary level. Ultimately, twisted ribbons may aggregate as in spherulites forming chiral objects, the quaternary level. But, as Bernauer astutely recognized, the optical activity of components is not a precondition for twisting.[1] Crystals of any point or space symmetry can twist. No direct relationship between molecular or crystallographic chirality and sense of twisting should be expected—it was long ago recognized that twisting in crystals has nothing to do with the presence or absence of crystallographic screw axes[226]—although correlations between configuration and crystallographic point symmetry with twist sense can be identified in some systems.[172]

4.3.1 Chiral Molecules

In a few instances, mesoscale twisting can be linked directly to the atomic configuration of the chiral, crystallizing molecules. Poly(*R*- and *S*-epichlorohydrin)[161,162] and poly(*R*- and *S*-propylene oxide) give right- and left-handed twisting, respectively.[149,161] Poly(D- and L-lactic acid) form left-handed and right-handed twisted crystals, respectively.[134] Enantiopure polymers such as poly(*R*-3-hydroxybutyrate) from bacterial sources always twist in one direction, in this case to the left.[161] Presumably the enantiomer will twist to the right. However, in this area of chemistry, as with so many others (e.g. optical activity, asymmetric synthesis), there is no simple correlation between molecular configuration and bulk manifestations of dissymmetry. Correlations between molecular configuration and sense of twisting failed for poly(3-hydroxyvalerate)[161] but this may be a consequence of the fact that the twist sense changes when the crystallographic twisting axis also changes.[267] Admixtures of just three percent of (*R*)-3-hexanoate chains instead of (*R*)-3-butyrate

chains in poly(*R*-3-hydroxybutyrate) can change the handedness of the resulting twisted crystals (Figure 17).[152] Small differences in molecular structure can change the sense of twist, as for the polyester (*R*)-(−)-4′-{ω-[2-(*p*-hydroxy-*o*-nitrophenyloxy)-1-propyloxy]-1-alkyloxy}-4-biphenylcarboxylic acid.[172] The number of methylene units in the chain backbone $n = 7$–11 determines the sense: if n is odd, twisted crystals are right-handed; if n is even they are left-handed.

4.3.2. Chiral Additives

In some cases, the sense of mesoscale twisting can be correlated to the configuration of chiral additives. For example, D- or L-tartaric acid added to polymorphs of resorcinol,[11] hydroquinone, malonamide, and glycolic acid, induces enantiomorphous twists, whereas racemic tartaric acid does not induce twisting at all.[73,74] Potassium dichromate forms equal fractions of right- and left-handed twisted crystals if grown from gel without additives but gives preferably right- and left-handed helices, respectively, in the presence of L- or D-aspartic acid or L- or D-glutamic acid.[30,205]

Recently, researchers claimed to control mesoscale twisting of crystallites induced by chiral additives.[278,279] However, Kunz and co-workers showed that the calcite helices detected by SEM[278,279] closely resembled ubiquitous scrapings of plastic laboratory equipment, underscoring the need to show representative micrographs and not only the most extraordinary form in a collection.[280]

4.3.3. Enantiomorphous Crystals

Enantiomorphs should twist in opposite directions. However, quartz is the only substance for which this relationship has been directly verified.[219] Hippuric acid ($P2_12_12_1$) twists in both directions in spherulites but twist sense has not been correlated with absolute structure. Optically pure twisted crystals from Bernauer that we have not reinvestigated include cocaine hydrogen chloride, santonin, cinchonine, rhamnose monohydrate, cholesterol monohydrate, menthol, formyl leucine, formyl valine, and asparagine hydrogen chloride.[1]

4.3.4. Enantiopolar Growth Directions

Brauns[226] and Bernauer[1] recognized that enantiomorphism is not a precondition for twisting. Twisted, tetragonal tetraphenyl lead crystallizes in the achiral point group $\bar{4}2m$. The [100] and [010] directions about which the crystals twist are enantiomorphous and both senses of twist can be found. Oxalic acid dihydrate crystals ($P2_1/n$) form right- or left-handed helices if growth occurs in the [010] or $[0\bar{1}0]$ directions, respectively, from a seed crystal. However, if both $\langle 010 \rangle$ directions grow simultaneously they twist in opposite directions forming a saddle-like morphology. Aspirin is centrosymmetric ($P2_1/c$) and the opposite ends of $\langle 010 \rangle$ elongated fibers are characterized by different twist senses (Figure 18c,d).[13] Ferrous muscovite ($C2/c$) grows as conical c^* elongated crystals with a convex (001) surface bent around the [100] and [010] axes. Rarely, crystals grow in both $\pm c^*$ directions forming two convex planes.[228] High-density polyethylene grows likewise, twisting in opposite directions for growth in opposite directions along the b axis. The sense of chain tilt with respect to the lamella normal determines the sense of twist.[127] Radial disclinations that interrupt circular bands sometime mark the boundaries between right and left twisting sections of poly(ε-caprolactone)/poly(vinyl butyral) blends.[145] We detected a similar coexistence of domains with right and left twisted fibers within the same hippuric acid spherulite.

In summary, crystals of any space group can twist. There is no direct correlation between molecular or crystal chirality and the ability of a particular substance to twist. Only in selected cases do we know with certainty that crystal chirality or the chirality of additives control twist sense. Crystals cannot twist along directions that are parallel to a mirror plane. If a mirror plane is perpendicular to the direction of twisting, the opposite ends of the crystal will show opposite senses of twisting. In the absence of a symmetry operation of the second kind (reflection, inversion, improper rotation), the sense of twisting will be the same for both ends of the crystal.

4.4. Intensity and Nature of Deformation

Crystallite size and pitch are strongly correlated. Pitch can change more than six orders of magnitude with the smallest cross-section dimension, h. A plot of $P(h)$ versus h is given in Figure 20. The upper bounds of the lines are not meaningful as very large pitches cannot be detected for crystals of finite size. Most banded spherulites reported are smaller than 2 cm,

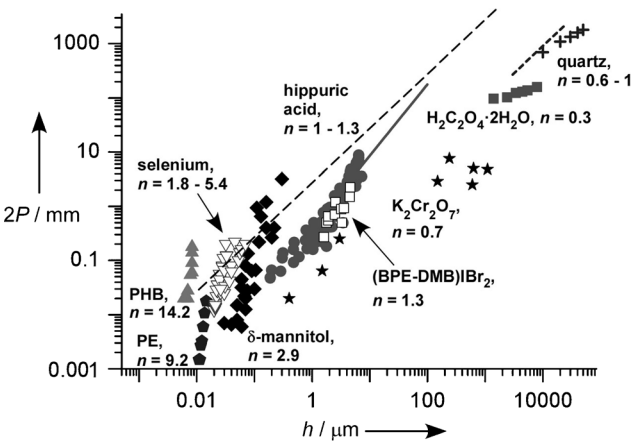

Figure 20. Correlation between full twist period ($2P$, 2π rotation, mm) and the smallest fiber size in a cross section (h, μm) for: quartz single crystals (-----[220] and +[219]), oxalic acid dihydrate, $H_2C_2O_4{\cdot}2H_2O$, single crystals (■),[219] potassium dichromate, $K_2Cr_2O_7$, single crystals[248] and open spherulites (★),[32] δ-mannitol spherulites, with 15 wt.% polyvinylpyrrolidone (◆),[105] hippuric acid single crystals (●[8,9] and ——[7]), (1,4-bis[2-(pyrene-1-yl)vinyl]-2,5-dimethylbenzene)IBr_2, (BPE-DMB)IBr_2, single crystalline ribbons (□),[198] two types of selenium spherulites (▽),[116,117] polyethylene spherulites, PE, 32 kDa (pentagons),[125] and poly(*R*)-3-hydroxybutyrate spherulites, PHB (▲).[148] The values of n are exponents in the fit $P = \text{const}\, h^n$. In the region below the dashed line, $2P < 10^3 \pi h$ or $\gamma_{max} > 0.001$, elastic stress in twisted crystals should relax, at least partially.

an approximate natural limit for twist periods detectable with an optical microscope. The lower bound corresponds to the maximum twist intensity for a given crystallite size h. For an elastically twisted rod or ribbon the maximum strain (γ_{max}) forms on the outer surface and approaches $\gamma_{max} = \pi h/(2P)$.[281] Similarly, for a bent crystal of curvature radius R, $\gamma_{max} = h/(2R)$. Estimates often give (Table 1, Figure 20) $\gamma_{max} > 0.001$ and sometimes $\gamma_{max} > 0.01$. Corresponding stresses can be estimated as $\tau_{max} = G\gamma_{max} > (10^{-3}–10^{-2})\,G$, where G is the shear modulus.

In micro- and macroscopic crystals ($h > 10$–100 nm), relaxation processes are driven by nucleation, and multiplication/motion of dislocations.[282–284] The yield strengths (τ_c) in ductile materials including metals, many molecular crystals, and ionic-covalent compounds forming at room temperature and melt-grown crystals forming at $T > (0.6–0.9)\,T_m$ fall in the range $\tau_c = (10^{-4}–10^{-5})\,G$.[283–286] Brittle materials fracture at critical stresses of approximately $10^{-3}\,G$.[287] Moreover, yield strength significantly decreases in the subsurface (several nm) layer[288–290] enhancing stress relaxation immediately after crystal growth. Comparisons of τ_c and τ_{max} shows that in most twisted crystals, elastic stress is partially or completely relaxed.

Plastic relaxation in macroscopic twisted crystals is evidenced by the following:

1) High dislocation densities[116] and well-developed mosaic block structure including microblocks (< 300 nm) and mesoblocks (2–200 μm) seen in X-ray diffraction rocking curves[219] and SEMs (Figure 3), as well as macroscopic blocks (> 0.2 mm) detected by eye (Figure 10b, 14c).[219,224,229,230,244–246,250]
2) Twisting variance over the cross section (Figure 16) and a correlation of twist intensity and density of mesoblocks (Figure 21).
3) Preservation of curved morphologies upon fragmentation of quartz, mica, oxalic acid dihydrate, potassium dichromate, and other macroscopic crystals,[219,250] as well as for micron-size crystals of hippuric acid.[9]
4) Low levels of residual elastic stress from anomalous biaxiality of twisted quartz.[219,222]
5) Large, facile, irreversible deformations of crystals induced by external forces such as gravity, or interactions with the container or other crystals.

In very small crystals, dislocation density can be low and yield strength high. Plastic deformation is unlikely, particularly at low growth temperatures ($T < (0.3–0.5)\,T_m$). This situation makes possible substantial elastic bending and twisting deformations as found in fibrous nano- and microcrystals grown from solution and the vapor, for example, ZnO nanoribbons,[185–187] and PbS and PbSe nanowires.[178,179]

Polymer lamellae are very thin ($h = 5$–20 nm) and usually grow from the melt at high temperatures, $T > 0.9\,T_m$. As corresponding yield strengths are high, approximately $\tau_c = (10^{-1}–10^{-2})\,G$,[291,292] only the strongest stresses can be expected to achieve twisting by plastic deformation (Table 1). Yet, plastic relaxation is evident in curved lamellar morphologies upon crystal fragmentation[293] and the formation of isochiral dislocations after crystal growth.[260] Irreversible plastic deformations in polymer crystals may result from molecular conformational relaxation.[294–296]

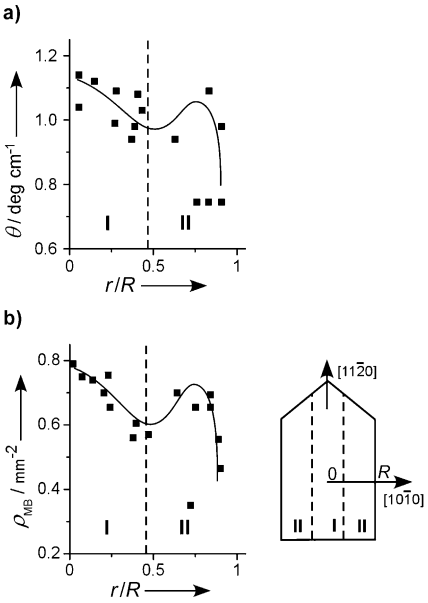

Figure 21. a) Inhomogeneity of twist intensity θ (°/cm) measured in a natural quartz crystal and b) density of mesoblocks ρ_{MB}, measured along the same direction.[219] The diagram on the right shows the location of the profile. Regions I and II correspond to two stages of quartz growth: along [11$\bar{2}$0] without and with thickening, respectively. Twist intensity was measured as the angular deviation of the optic axis outcrop from the normal to the crystal cut. Density of mesoblocks was calculated from broadening of X-ray diffraction reflections by the method of moments.

4.5. Untwisting

Single crystals grown under constant conditions show that the thicker the crystal, the greater the pitch (Figure 20). See also data on twisted PbS and PbSe nanowires,[178,179] bent ZnO nanobelts,[188] and twisted ribbons of 9-anthracenecarboxylic acid.[21] Fitting these data to a power law $P \propto h^n$ gives $n = 0.3$–14.2; most data conform to $n = 0.6$–1.3.

This behavior is intuitive. Increased rigidity of a thickening crystal will resist the twist moment applied to the crystal whether the forces are internal or external. In a rod twisted by a torque or a twist moment, M, the half twist period (π rotation) is expressed as $P = \pi/\theta = \pi GJ/M$, where G is the shear modulus and J is the torsion constant.[281] For a circular rod of radius r, $J = \pi r^4/2$. For non-circular cross sections, the geometric dependence becomes more complicated but the proportionality $J \propto r^4 \propto h^4$ holds leading to $P(r) \propto r^4 M(r)$. Although $M(r)$ is specific for every case and, in general, unknown, the functional dependence can be estimated for the main distributions of twisting stress—twisting forces are applied along some line (e.g. the line of axial dislocation) or some surface (outer surface, sector zoning boundaries). In the cross section, stress sources correspond to points and lines leading to $M \propto r^2$ and $M \propto r^3$, respectively. Thus, in $P \propto h^n$ the

exponent n should range from 1 to 2. However, this analysis does not involve the plastic relaxation of the deformation.

As shown for large quartz crystals,[219] smaller gypsum crystals,[219,244] micron-sized needles of hippuric acid,[8,9] and δ-mannitol fibrils in spherulites,[105] twisting and bending begins at the crystal tip. As a rod thickens, crystals untwist and pitch increases. This was also seen in helices and helicoids of chiral amphiphiles.[297] Twisting is a dynamic process and the coexistence of variously twisted segments of a single crystal is not a consequence of equilibrium processes,[298] but rather growth history.[8,219] Untwisting was observed in situ for gypsum[219,244] and oxalic acid dihydrate[219,253] growing in solution, as well as for hippuric acid[8] (Figure 22) and δ-mannitol[105] growing from the melt. Post-growth observations suggest untwisting for quartz[219,222] and vapor-grown hippuric acid.[9] A crystal constrained by adhesion to the substrate surface (Figure 23a) or to other crystals, or by confinement between walls of the chamber,[8] may not untwist, and thus it may have a much smaller pitch (Figure 23a) than an unencumbered crystal (Figure 23b). Strongly twisted, free-standing, or freely suspended crystals can untwist almost completely as for melt-grown hippuric acid needles.[8] Thin plates of 2,5-di-*tert*-butyl-1,4-dimethoxybenzene show complex curling and uncurling behavior during growth from acetic acid solution, behavior which is analogous to twisting and untwisting.[200]

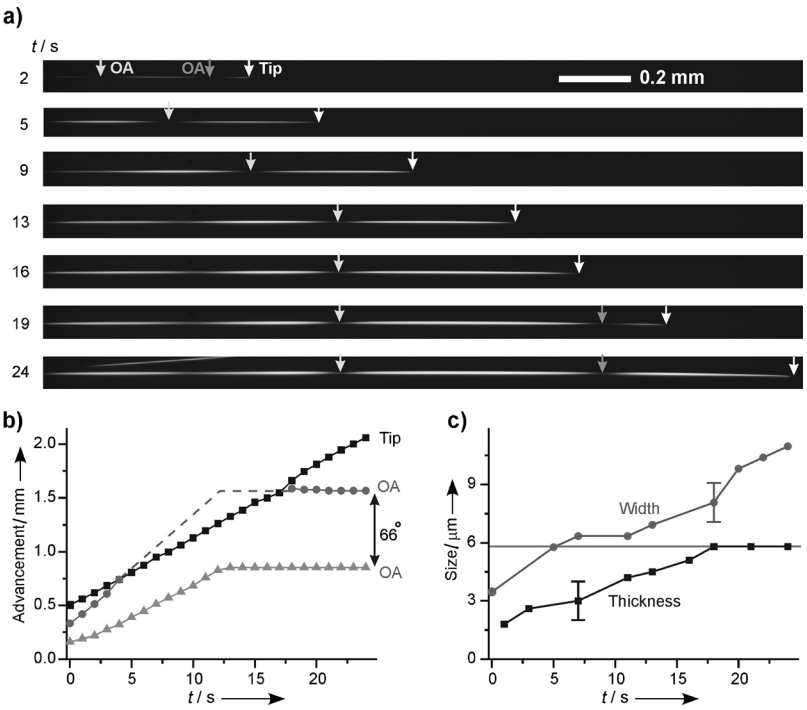

Figure 22. a) A sequence of images between crossed polarizers showing the evolution of a hippuric acid needle grown from the melt. "OA" marks those spots where an optic axis is perpendicular to the slide surface. b) The advancement of a hippuric acid tip and two OAs as a function of growth time. c) Averaged needle width and thickness as a function of growth time. Horizontal line shows thickness of the melt layer between glasses. The distance between OAs increases (twist intensity decreases) as long the as crystal surface is surrounded by the melt and not obstructed by the container. Reproduced from Ref. [8] with permission.

Since deformation is essentially plastic, the theoretical $P(r)$ dependence should involve not only the expression for $M(r)$ but also stress relaxation processes occurring during crystal growth. A beautiful illustration of this was provided by Shaskol'skaya and Pashkov[299] who plastically bent a single-crystalline rock-salt plate. During subsequent growth and thickening in a supersaturated salt solution, the imposed deformation of the plate was undone.

No theory, to our knowledge, has been elaborated to account for the plastic relaxation of twisted crystals. Analyses of experimental $P(r)$ dependences always invoke purely elastic criteria appropriate only for nanocrystals growing far below the melting point (Section 4.4). As a first step, a twist moment only at the crystal tip can be considered. Immediately after growth, elastic stress relaxes completely resulting in a plastically twisted internal core with the twist period $P_0 = \pi/\theta_{p,0}$ and the cross-section size h_0 or $2r_0$ (Figure 24). The crystal then thickens as new material is attached to the lateral surfaces that are already distorted by the twisted core. Because the sides are curved, newly deposited layers become stressed and try to untwist (unbend) the core.

Untwisting can be simulated on the basis of some reasonable assumptions. A simple model assumes that the crystal grows by elementary layers and stress relaxation in the surface i^{th} layer occurs as long as this layer is not buried by successive layers. At any time, the total twist, $\theta_T = \pi/P$, consisting of elastic ($\theta_e = \gamma_e r$) and plastic ($\theta_p = \gamma_p r$) contributions remains constant over the whole crystal, $\theta_T = \theta_{e,i} + \theta_{p,i} =$ const, $i = 1,\ldots N$. The mechanical equilibrium condition for a crystal consisting of N layers requires that the total twist moment is zero [Eq. (1)].[281]

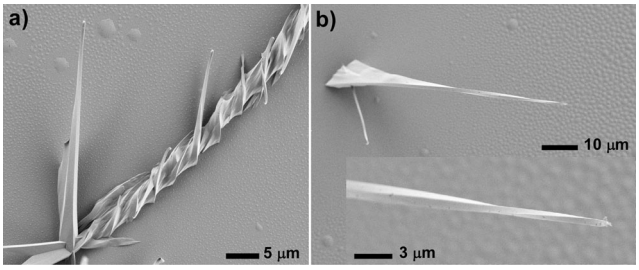

Figure 23. Scanning electron micrographs of hippuric acid needles grown from the vapor at 210 °C.[9] a) The crystal attached to a glass substrate shows a strong twisting, $P = 8$ μm. This value corresponds to the typical twist intensity at the crystal tip and shows no evidence of untwisting. Free standing branches of the same crystal show much larger pitches. b) Crystal grown perpendicular to the substrate and showing inhomogeneous twist intensity. Near the base $P > 500$ μm while near the crystal tip $P < 15$ μm. Inset shows an enlarged image of the crystal tip.

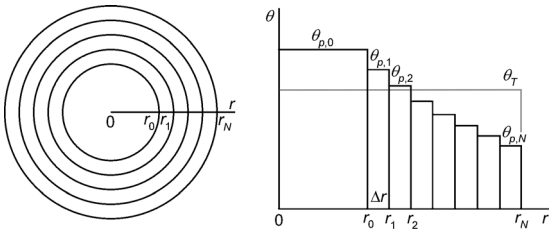

Figure 24. Diagram illustrating the distribution of plastic and total twist intensity along radius of a thickening rod.

$$M = \sum_{i=0}^{N} M_i = \sum_{i=0}^{N} GJ_i\theta_{e,i} = 0 \quad (1)$$

If plastic relaxation accommodates all the stress immediately, the twist period does not change and $P(r) = P_0$ (line 1 in Figure 25). In the opposite limit, there is no relaxation and $P(r) = P_0(r/r_0)^4$ (line 2 in Figure 25). The experimental data (Figure 25) lie between these limits and suggest partial stress relaxation.

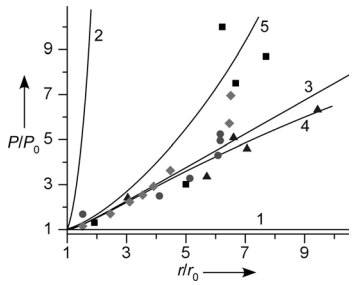

Figure 25. P/P_0 as a function of r/r_0 for four needle-like hippuric acid crystals,[9] distinguished by four symbols. Twist period, P, and crystal thickness, h, and width, H, determined by SEMs. Values of P, h, and H measured at the crystal tips were used as initial values (marked by subscript 0) prior to untwisting. The effective radius of the cross section, r, was recalculated from h and H assuming the constancy of a torsion constant $J = \pi r^4/2 = (0.332H - 0.203h)h^3$.[281,300] Solid lines show different stress relaxation regimes. 1) Immediate and complete plastic stress relaxation; 2) No stress relaxation; 3)–5) Simulations using the relaxation model described in Section 4.5. 3) $\alpha = 1$; 4) Fit to triangles, $\alpha = 0.9998$; 5) Fit to squares, $\alpha = 1.000025$.

The condition for plastic relaxation can be introduced in several ways. In the simplest case, some fraction α of defects that create plastic strain in the underlying layer emerges in the new layer, $\gamma_{p,i} = \gamma_{p,i-1}\alpha$, $i = 1,\ldots N$, where $\gamma_{p,0} = \theta_{p,0}r_0 = \pi r_0/P_0$ is the plastic strain at the crystal tip. If all defects from the core penetrate the new layer ($\alpha = 1$), the agreement between theory and experiment is excellent for all points with $r/r_0 < 6$ (line 3 in Figure 25). For the whole data range, the agreement can be improved by slight variations of α (lines 4 and 5 in Figure 25).

The model described above assumes smoothly varying deformations across the whole crystal. This may not be the case for very large twisted quartz and mica that might have discontinuities between concentric twisted and untwisted volumes (Figure 24). Outer layers, acting to untwist the core, could well separate from it by cracking or intensive plastic deformations. Stresses developed during untwisting are manifest in crystal cracking. Cracks can form in the outer layers (gypsum[219]) and in the crystal core (quartz[219]).

4.6. Effect of Composition, Additives, and Growth Conditions

Bending and twisting can be controlled by the crystal composition. Sometimes for a series of isomorphous compounds only specific compositions show curved morphologies. For example, our experiments demonstrate that among a large number of Tutton salts, $A_2Me(SO_4)_2{\cdot}6H_2O$, and their solid solutions growing from aqueous solutions, only $(NH_4)_2Cu(SO_4)_2{\cdot}6H_2O$ and $(NH_4)_2(Co,Fe)(SO_4)_2{\cdot}6H_2O$ form spontaneously bent crystals. A variety of micas can be found in pegmatite veins but only ferrous muscovites, some lepidolites, and rarely biotites bend.[228–230]

Twisting of many of Bernauer's small molecules was encouraged by the addition of various natural resins. A qualitative relationship between twisting in cholesterol with the additive santonic acid was described by Gaubert.[81] A quantitative relationship between impurity concentration and twist intensity was established for oxalic acid dihydrate grown from water/acetone mixtures,[219] aspirin spherulites grown with salicylic acid,[13] mannitol with polyvinylpyrrolidone (Figure 26a),[105] poly(butylene succinate) with poly(ethylene

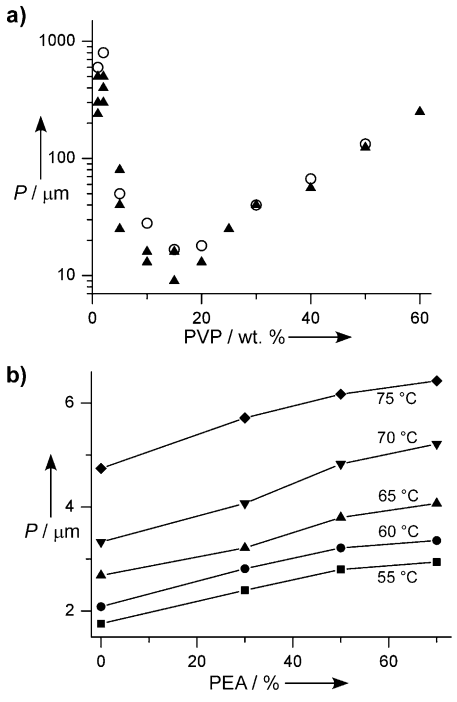

Figure 26. Twist period, P, for fibers in melt grown spherulites as a function of additive concentration. a) δ-Mannitol with polyvinylpyrrolidone (PVP); triangles correspond to growth at 110 °C and circles to growth at 115 °C. Reproduced from Ref. [105] with permission. b) Poly(butylene succinate) blended with poly(ethylene adipate) (PEA) Growth temperatures are indicated near the corresponding curves. Replotted from Ref. [140] with permission.

adipate) (Figure 26b),[140] poly(3-hydroxybutyrate) with poly(3-hydroxyhexanoate) and poly(3-hydroxyvalerate),[152] and poly(ε-caprolactone) with poly(vinyl butyral).[156] Zn and Hg vapors induce twisting in sulfur spherulite fibers,[115] Mg^{2+} and Cd^{2+} affect bending of gypsum crystals.[244,245,247]

Impurities can intimately direct twisting so that the result is stereospecific as found for resorcinol, glycolic acid, hydroquinone, and malonamide each with D- and L-tartaric acid.[11,74,75] In all these cases, the impurity is presumed to work, in part, through solid-solution formation (see Section 5.7).

Impurities can also affect pitch indirectly by modifying crystal morphology, reducing crystallite size, altering the packing of fibrils, or suppressing growth below threshold supercoolings and supersaturations. Probably resins and polymers added produce ring-banded spherulites in this way. Poly(ethylene adipate) increases the band spacing in poly(butylene succinate) (Figure 26b).[140] Atactic poly(lactic acid) and atactic poly(3-hydroxybutyrate) intensify twisting in poly(L-lactic acid).[120] A poly(ethylene glycol) admixture promotes banding in poly(L-lactic acid) and poly(D-lactic acid).[134]

The separation of multiple twisting influences has not been cleanly achieved. Tetraphenyl lead does not form twisted crystals without the addition of polyvinylpyrrolidone (PVP) or a natural resin in an amount greater than 5–10 wt.%.[6] This necessity may be a direct chemical consequence of the disruption of the host lattice by the macromolecular additive, or the PVP may achieve higher supercoolings of the melt thus increasing the driving force for crystallization. Thus, it is not clear if PVP works directly by host/guest interactions of some kind, or merely suppresses growth until high supersaturations can be achieved, or both. PVP induces twisting of mannitol fibers if added in small amount (Figure 26a). Oxalic acid dihydrate forms twisted crystals from acetic acid or acetone but not water.[219,253,254] Incorporation of 0.01–0.03 wt.% of acetic acid and acetone may be directly responsible for twisting,[255] but, on the other hand, solvents effect habit thereby altering the size and shape of growth sectors and the distribution of mismatch stresses between them.[219,228]

Remarkably, the distinction between chemically direct and indirect additive effects was already presupposed by Wallerant in 1906.[74,75] He reported that while (−)-santonic acid induces left-handed twisting in crystals of malonamide (and *p*-azooxyanisole), and the pitch tightens with increasing santonic acid concentration, the refractive indices of the malonamide crystals are essentially unchanged up to 33 wt.% additive. Wallerant supposed that, in this case, as opposed to some others, santonic acid was not inside the crystals but rather between the fibrils.

For most spherulite fibers crystallizing from the melt, the twist period decreases as temperature drops or supercooling (ΔT) increases. Examples include, but are not limited to: hippuric acid,[6] tetraphenyl lead (Figure 1f) and tetraphenyl tin,[6] mannitol,[105] testosterone propionate,[10] resorcinol,[11] aspirin (Figure 1c), selenium,[117] poly(ethylenes),[124,125,133] poly(ethylene terephthalate),[100,121] poly(lactic acid),[120,160] poly(3-hydroxybutyrate),[148,150] poly(butylene succinate),[140] poly(epichlorohydrin),[162] α-poly(vinylidene fluoride),[141,166] polystyrene and poly(L-lactic acid) block co-polymer blended with poly(ε-caprolactone) or poly(D-lactic acid),[169] polystyrene-b-poly(L-lactic acid),[169] and poly(trimethylene terephthalate).[142] Fitting data to a power function, $P \approx (\Delta T)^{-n}$ reveals exponents n ranging from 1 to 8 (a portion of the data is summarized in Table 1 from Ref. [8]). Since fiber thickness also decreases as supercooling increases, it was tempting to use $P(\Delta T)$ behavior to find a functional form of $P(r)$ dependence and exploit it for verification of the twisting mechanisms.[133,138,151] Such attempts are not valid because they rely on a weak assumption of a constant driving force for twisting with temperature and does not account for inevitable plastic relaxation (Section 4.5). Moreover, detailed examination shows that $P(\Delta T)$ dependence usually does not fit a power function in the whole temperature range and sometimes $P(\Delta T)$ has a minimum[142,150] or a maximum.[10,105] Crystallization from the melt is characterized by the twofold action of ΔT; it is a measure of driving force for growth (supercooling) and the absolute temperature itself. These two influences are hard to separate. The "pure" effect of temperature only can be observed for the growth from the solution and vapor phases.

For single crystals we have less data. Dolomite shows a specific saddle morphology at higher temperatures.[233,235] Vapor-grown hippuric acid needles[9] have a constant pitch over the temperature from 30 °C to 140 °C ($T_m = 188$ °C).

Little is known about the effects of other growth parameters. Higher supersaturation seems to promote twisting of oxalic acid dihydrate from acetone[219,253] but inhibit it if grown from acetic acid.[255] Gypsum bending decreases as supersaturation increases.[244,245,247] The effect of supersaturation and growth temperature on the twist intensity can be complex because of numerous indirect relationships (such as, change of impurity uptake, growth rate and aspect ratios, mass transfer).

5. Mechanisms

The principle of Occam (that the best hypothesis is simplest one, or the one based on fewest assumptions) will naturally drive our discussion of mechanism in search of a single, universal, twisting/bending mechanism. At the same time, we recognize that an insistence on a "one-size-fits-all" explanation may be foolhardy. The substances we are discussing span great ranges of chemical composition, size and shape, physical properties, and growth conditions. There are many ways to twist a rod or a plank and in individual cases, more than one force may be operative. These choices may be narrowed with discerning experiments. However, in our experience, when a variety of explanations compete to explain symptoms that are expressed throughout the crystal kingdom, each credible idea is right some of the time for some substances under some conditions.

5.1. Surface and Space Charge and Spontaneous Polarization

ZnO, GaN, and AlN nanoribbons[185,189,191] with polar wurtzite-like crystal structures ($P6_3mc$) develop broad {0001} faces. Similar nanoribbons are observed for polar surfaces of cubic ($F\bar{4}3m$) InP,[195] tetragonal ($P4_2/mnm$) SnO_2,[197] and monoclinic ($C2/m$) $Ag_2V_4O_{11}$.[196] Surface charge can bend these ribbons by minimizing electrostatic energy at the expense of elastic energy or by distortive consequences of the inverse piezoelectric effect. Quantitative models of $R(h)$ dependence on surface charging have been developed.[185,186,188,191,193] Models of twisting based on electrostatics and piezoelectricity are restricted to a narrow class of nanocrystals of suitable morphology with polar surfaces. They cannot apply to centrosymmetric SnO_2 and $Ag_2V_4O_{11}$. It has been suggested that macroscopic quartz-crystal twisting is due to pyroelectricity,[220] but we are skeptical.

5.2. Isochiral Transverse Screw Dislocations

Arrays of isochiral screw dislocations in polymer lamellae (Figure 27 b) have been argued as the cause of twisting.[164,301] Such dislocations give incremental displacements periodically as opposed to a continuous twist (Figure 27 a). Model

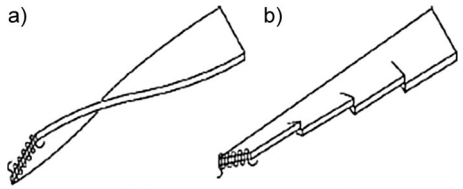

Figure 27. a) Continuous versus b) discontinuous twisting in polymer lamella. Crystal in (b) is punctuated by isochiral screw dislocations. Reproduced from Ref. [124] with permission.

calculations carried out for a series of identical giant dislocations with Burgers vector equal to the thickness of the layers (ca. 10 nm) which are evenly distributed along the lamella's midline, provide reasonable twist periods.[301] Although dislocations of this kind abound,[164,165,302] comparable twisting was observed even in their absence.[276] This situation may imply that dislocations are not the cause but rather a consequence of twisting in some cases, a mechanism of stress relaxation (Section 4.4). Suspicion is engendered by the fact that giant dislocations often appear near the lamella reentrant angles[302] or are associated with the branching points.[303] Moreover, the stochastic processes of dislocation nucleation would likely produce very inhomogeneous twisting. Although lamellar twisting may not be constant within and between neighboring crystals, it is not stochastic; ring-banded spherulites are characterized by rhythmic, in-phase organization (Sections 4.1, 4.2). In any case, the giant dislocation mechanism can be applied, at best, to thin ($h <$ 50 nm), ribbon-like crystals. Thicker crystals require many dislocations with extremely large Burgers vectors.

5.3. Eshelby Twist

Axial screw dislocations may create elastic stress fields that twist crystals.[304] The twist angle $\theta = \pi/P = kb/A$, where b is the magnitude of the Burgers vector, A is the cross-sectional area, and k is a geometrical constant close to unity ($k = 1$ for an ellipse).[305] The screw dislocation was made vivid in cuprite.[306] Formation of axial screw dislocations in whiskers is possible for some growth regimes when new layers constantly nucleate around a screw dislocation according to the classical dislocation-spiral mechanism[14] but do not spread in the lateral directions because of impurity poisoning of the growth steps. Eshelby's mechanism has been applied to fibrous crystals (LiF,[181] NaCl,[182] Hg,[307] Sn,[206] Pd,[207,208] Al_2O_3,[209,210] among others) since 1950. Recently, confirmations of this mechanism on the nanoscale for PbSe,[179] PbS,[178] and ZnS[211] has given added weight to Eshelby's prescient insights (Figure 28). Nevertheless, the Eshelby mechanism

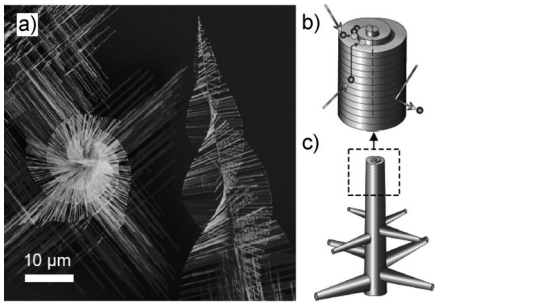

Figure 28. a) PbS nanowires grown by the Eshelby mechanism. b) Schematic illustration of axial screw dislocation at the tip of the trunk in c) that further illustrates the displacement of lateral branches. Reproduced from Ref. [178] with permission.

was likely overextended to ribbon-like crystals of (1,4-bis[2-(pyrene-1-yl)vinyl]-2,5-dimethylbenzene)IBr_2[198] and lithium 12-hydroxystearate[176] that show strong impurity control of twisting.[176,177] Eshelby twisting is not a universal mechanism.

For spherulite fibers, the presence of axial screw dislocations is questionable. Even if such dislocations form, the ensemble of dislocations should not be the same for thousands of fibers in each spherulite and hundreds of different spherulites forming in the same sample. Moreover, branching of individual fibers, which is definitely related to dislocation structure, does not strongly affect pitch. For bigger crystals, Eshelby twist is unobservable because it predicts large pitches for sensible Burgers vectors (e.g. $P = 50$ m for $r = 0.1$ mm and $b = 1$ nm). Detection of such weak twisting is impossible with standard crystal optical and electron microscopic techniques but it can be assayed by X-ray diffraction topography. For example, for ZnS whiskers, this method established $P \approx 10$ m.[211]

5.4. Twinning

Sometimes twisted crystals are composed of mis-oriented plates resembling complex twins. This mechanism of twisting

was championed by Imai and Oaki for potassium dichromate (Figure 3),[202–205] orthoboric acid,[32,202–204] potassium sulfate,[308] and D- and L-aspartic acids,[30,31] pyrene,[309] and copper sulfate pentahydrate.[310] In these systems, twins are invariably and improbably offset by small amounts (3–12°) but the corresponding twin laws have not been identified for any of these compounds. Oaki and Imai suggested that misorientations arise from fields around the growing crystal (see Section 5.5). This idea emerged from the literature on banding in high-polymer spherulites. In addition, others proposed a twinning-to-twisting scheme[311,312] for helical quartz crystals and chalcedony fibers riddled with Brazil twins. However, silica crystals can be twisted but not twinned and vice versa. More probably, both twinning and twisting are unrelated mechanisms of stress relaxation.[219]

5.5. Fields

Several types of fields can form around crystallizing materials including the following: 1) thermal fields from the latent heat of crystallization and temperature gradients from inhomogeneous sources of heat; 2) mechanical fields from density variations between the crystal and melt; and 3) compositional fields from the concentration of impurities in the melt by the growing crystal. Fields can generate forces on a growing crystal that produce a twist.[313] This mechanism was assumed to induce twisting in potassium dichromate,[32,205] orthoboric acid,[30,32] potassium sulfate,[308] D- and L-aspartic acids,[30,31] hippuric acid,[7] polyethylene,[124,125] poly(vinylidene fluoride),[166] and polymer lamellae, generally.[7,314]

Strong temperature gradients are responsible for curved morphologies in many crystals growing near the melting point,[14,27] and for metal lamellae forming during eutectic crystallization.[212–214] Such phenomena are not considered herein (see Section 1), but strictly speaking they are manifestations of field mechanisms. In most cases of bending and twisting they are not likely to be meaningful.

Toda associated polymer twisting with Mullins–Sekerka-like instabilities, planar growth front instabilities induced by competition between mass/heat transfer and attachment of growth units to a crystal.[124,125,166] Branching events that control lamella width are expected to be proportional to $(D/V)^{0.5}$, where D is the diffusion coefficient in the melt and V is the growth rate. The proportionality of P to the aforementioned quantity $(D/V)^{0.5}$ was taken as evidence of the mechanism. This weak evidence can be contradicted:

1) Fine fibers in compact spherulites and isolated single fibrous crystals can grow under similar conditions and show similar twist periods despite principally different mass and heat transport conditions (hippuric acid,[6] mannitol[105]). The same relates to spherulites growing at different temperatures with similar twist intensities (hippuric acid[6]). Poly(ethylene) and poly(3-hydroxybutyrate) lamellae are twisted if they grow from the melt[133,151] or from solution.[151,170]
2) Minor impurities can strongly affect twisting but not fields. Melt-grown resorcinol spherulites formed in the presence of tartaric acid provide a nice example. Fibers are not twisted if 10 wt.% racemic tartaric acid is added to the melt, but if the tartaric acid is in enantiomeric excess of 0.1% *ee*, banded spherulites form.
3) Spherulitic growth is typically interface controlled[12] under conditions of low temperature and concentration gradients.
4) Twisted crystals (gypsum, oxalic acid dihydrate, quartz, dolomite) can grow from non-viscous solutions that suppress strong fields. Likewise, fields do not form in the vapor phase, the growth medium for twisted hippuric acid crystals.
5) External forces required to twist large crystals (>1 mm) should be impossibly large.

5.6. Surface Stress

Unbalanced surface stress is arguably the best-articulated mechanism for lamellar twisting and bending in high polymers. Surfaces differ from the crystal interior in the arrangement of molecules, lattice constants, and sometimes in chemical composition. Such differences induce stress that can relax by means of macroscopic crystal twisting as for a trimetallic strip, composed of one metal strip sandwiched between two strips of another metal, that is subject to a change in temperature. Surface stress as a twisting mechanism was first proposed by Lehmann[60] and similar ideas were subsequently formulated.[26,315] In the 1980s, surface stress proliferated as the cause of polymer-lamellae twisting.[99,122,129,133,152,267,276]

Polymer lamellae are thin (5–20 nm). Nevertheless, they have comparatively thick, ill-defined (>0.5 nm) surface layers characterized by folded chains. These layers have anisotropic structures, elasticities,[316] and surface energies.[317] However, the presence of anisotropic surface stress is not sufficient for a macroscopic deformation. Indeed, if the stress distribution is the same on the lower and upper surfaces of a lamella, no twist moment is generated. To induce twisting the stress must be unbalanced. To date, most researchers have considered orthorhombic or monoclinic polymers, such as poly(ethylene), poly(3-hydroxybutyrate), poly(3-hydroxyvalerate), poly(lactic acid), or α-poly(vinylidene fluoride), growing along their twofold axes. The lamellae are wedge-like and consist of two growth sectors formed by {110} faces (Figure 29a,c).

The imbalance is expected to come about in one of two general ways. The classic proposal by Keith and Padden[129] for poly(ethylene) and for α-poly(vinylidene fluoride) ascribes the imbalance to polymer chains tilted with respect to the folding surface[99,129,133] (Figure 29b). The upper folding surface (h01) ($h=2$, 3, sometimes 1) makes an obtuse angle with the (110) growth face and an acute angle with the $(\bar{1}10)$ growth face. In accordance with the twofold symmetry, the $(\bar{h}0l)$ surface makes an acute angle with the (110) growth face and an obtuse angle with the $(\bar{1}10)$ growth face. Such a difference can be a precondition for the folding differences on the (h01) and $(\bar{h}01)$ surfaces of the {110} growth sectors (halves of the lamellae) and different surface stresses. The difference in surface stresses on the upper and lower sides of

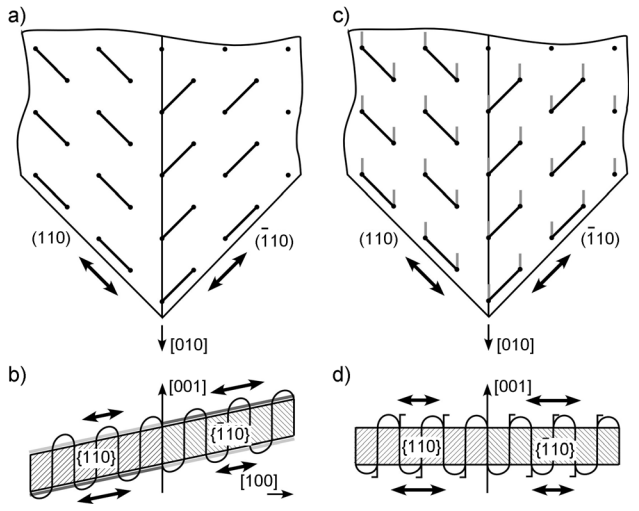

Figure 29. Formation of unbalanced surface stress in polymer lamella growing along a twofold axis [010] and consisting of two {110} growth sectors linked together along the central line. Such a lamellar structure is common for many polymers including poly(ethylene),[133] poly(3-hydroxybutyrate),[138] poly(3-hydroxyvalerate),[267,319] poly(lactic acid),[134,320] or α-poly(vinylidene fluoride).[133] a) and b) Achiral polymers, such as poly(ethylene), with folding surface (*h*01); c) and d) Chiral polymers, such as poly(3-hydroxyvalerate) or poly(lactic acid), with folding surface (001). a) and c) Top view. Dashes show orientation of polymer chains in the folding surface. Directions of largest surface stresses shown by double arrows. Gray dashes in (c) symbolize orientation of the functional groups on the lamella surface. b) and d) View down twofold axis. Double arrows show difference in the surface stresses on the folding surfaces. Hatching highlights different orientation of {110} faces. b) Non-equivalence between upper and lower half surfaces is due to the tilt of molecules with respect to the basal plane in achiral polymers. Acute and obtuse angles between corresponding {*h*01} and {110} surfaces shown by gray and light gray lines, respectively. d) Non-equivalence in chiral polymers is due to the different arrangement of functional groups (schematically shown by Γ-like symbols) with respect to the chain fold directions.

each half lamella, bend the growth sectors in opposite directions. However, as the growth sectors form a continuous elastic body, twisting redistributes the stress. The stress distribution results in coiling if one growth sector is dominant.[99,318] Correlations of chain tilt and twist sense support this idea.[127] If the chains tilt clockwise from the normal to the lamellar basal plane—looking along the growth [010] direction toward the crystal nucleus—they form a right-handed helix, whereas lamella with the chains tilted counterclockwise are left-handed.

Basset criticized this hypothesis[122] by showing that lamellar twisting in poly(ethylene) occurs even if the folding surface is {001}, a surface that cannot provide unbalanced surface stresses, and it does not occur immediately during growth of the crystal tip but later during lamellar thickening.[132,260] He supposed that surface stress emerges only during reorganization of the folding surface.[122]

In chiral polymers, such as poly(*R*-3-hydroxybutyrate) or poly(*R*-3-hydroxyvalerate), the equivalence of the upper and lower surfaces is broken because the functional groups are differently oriented with respect to the folding direction.[152,267] In fact, orientation of the chiral functional groups with respect to the folding surfaces will be the same on upper {110} and lower $\{\bar{1}10\}$ surfaces as well as on upper $\{\bar{1}10\}$ and lower {110} surfaces, but different for upper and lower surfaces in the same growth sector (Figure 29c,d). This situation causes growth sectors to bend in different directions if they are separated and twisting of the whole lamella if the growth sectors form a continuous body.[155,276] Such a scheme of stress distribution is confirmed by the observation of lamella bending and coiling if one growth sector is morphologically dominant[155,276] (Figure 30), as well the observation of opposite twist sense for lamellae with the same folding surfaces {001} but growing in orthogonal (*a* vs. *b*) crystallographic directions.[276]

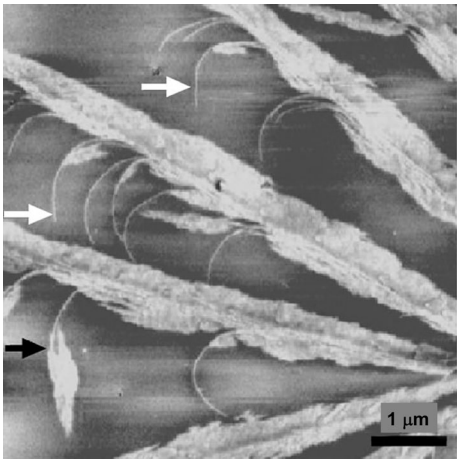

Figure 30. AFM of poly(*R*-3-hydroxybutyrate-co-17 mol%-*R*-3-hydroxyhexanoate) lamellae in its blended melt with atactic poly(3-hydroxybutyrate). The branches splitting from the main lamellae initially consist of one growth sector (half of lamella) and bend. As the second growth sector forms and becomes comparable in size the lamella start to twist. The white and black arrows indicate lamellar bending and twisting, respectively. Reproduced from Ref. [276] with permission.

Despite a clear crystallographic basis for lamellar twisting, quantitative support for this mechanism is lacking. The only confirmation is provided by the reasonable agreement between values of surface stresses simulated for polyethylene (-0.27 and $-0.4\,J\,m^{-2}$ for two orthogonal in-plane orientations)[317] and calculated on the basis of poly(*R*-3-hydroxybutyrate-co-*R*-3-hydroxyhexanoate) (0.1 and $-0.1\,J\,m^{-2}$) twisting.[152]

5.7. Heterometry Stress and Autodeformation

The autodeformation mechanism was proposed by Punin in the 1970s and 1980s to explain the formation of various crystal growth defects, such as bulk martensitic or diffusionless phase transformations, crystal bending and twisting, non-crystallographic branching, and growth twinning, among other peculiarities. With the exception of two brief Reviews

in English,[321,322] most of the relevant papers, and a book,[219] were only published in Russian. We have recently discussed the concept in relation to small-angle branching in spherulites (not necessarily banded spherulites).[11] Herein, we provide a brief summary of the autodeformation mechanism emphasizing its application to crystals that bend and twist during growth. This mechanism has been applied to macroscopic quartz,[219,222,254] mica,[228–230] gypsum,[244,246] and oxalic acid dihydrate[219,253,254] single crystals, as well as resorcinol,[11] hippuric acid,[8] and aspirin fibers[13] in banded spherulites.

Real crystals have spatial inhomogeneities in the distribution of impurities/additives. Sub-volumes that grew at different times frequently have different compositions as growth conditions change. This leads to concentric zoning, common in minerals. Symmetry-independent growth sectors would be expected to have compositional differences, intersectoral zoning. Spatial compositional inhomogeneity within a single growth sector is called intra-sectoral zoning. Compositional differences lead to local differences in lattice constants (heterometry), that results in strong elastic strain and stress. Internal stress can also appear as a result of an inhomogeneous temperature distribution or crystallization pressure, among other sources.

Stress relaxes by means of plastic and brittle deformations. Dislocations that nucleate and multiply can organize themselves into ensembles giving birth to misoriented blocks. Growth of blocks having preferable misorientations results in macroscopic bending and twisting. The process is akin to noncrystallographic branching.[11] Dislocation ensembles may serve as new sources of internal stress forming a positive feedback loop and resulting in autocatalytic process of defect multiplication.

α-Quartz advancing along its twofold axis $[11\bar{2}0]$ is the most closely studied example of growth-induced twisting.[219,222,254] Symmetry independent quartz growth sectors (Figure 31 a) are characterized by different Al^{3+} concentrations and attendant monovalent cations that substitute for silicon $Si^{4+} \leftarrow Al^{3+} + R^{+}$, R = Li, Na, H. γ-Ray irradiation produces Al color centers with a smoky coloration proportional to the Al^{3+} concentration and marking its distribution (Figure 31 a). Heterometry associated with differences in Al^{3+} concentration can be measured precisely in large quartz crystals (up to several cm).

In the plane of the crystal $(11\bar{2}0)$ cross section, both lattice constants *a* and *c* lie in the plane. For the growth sectors *R*, *r*, and *W*, either *a*, *c*, or *a* and *c* lattice constants are larger than the corresponding lattice constants in all other growth sectors (Figure 31 b). The condition of deformation consistency on the sectorial boundaries requires stretching of growth sectors *R*, *r*, and *W* in the cross-sectional plane with respect to others. Mismatch stress created by such deformations will create a twist moment in this plane (Figure 31 b). Levorotatory quartz crystals twist left, whereas dextrorotatory crystals twist right.

Along the growth direction or perpendicular to the $(11\bar{2}0)$ cross section there is only one lattice constant, *a*, which is larger in the *R*, *r*, *m*, and *W* growth sectors than in others (Figure 31 c). This is a consequence of tension in *R*, *r*, *m*, and *W* that causes compression of other growth sectors. Twisting and deplaning occur because of the consistency of deformations on the sector zoning boundaries and the absence of normal stress components (that is, stress components directed perpendicular to a surface of a given crystal volume) on the crystal surface (Figure 31 c).

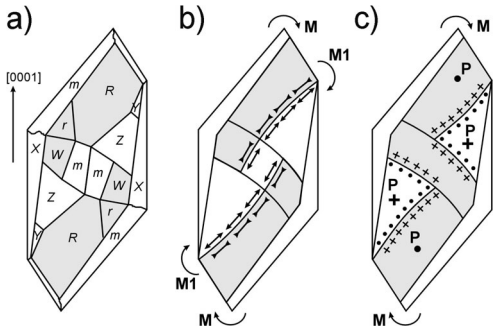

Figure 31. Creation of macroscopic twist moments, **M**, in the right-handed quartz crystal.[219,254] a) Distribution of growth sectors in the quartz cross sections cut normal to the growth $[11\bar{2}0]$ direction. Growth sectors: $R=\{10\bar{1}1\}$; $r=\{01\bar{1}1\}$; $m=\{10\bar{1}0\}$; $Y=\{21\bar{3}1\}$; $Z=\{41\bar{5}1\}$; $W=\{\bar{1}0.18.1\}$; $X=\{51\bar{6}1\}$. Gray corresponds to stronger intensity of radiation-induced coloration. b) Twist moments, **M1**, created by composition inhomogeneities in the cross section. In gray growth sectors both lattice constants *a* and *c* are greater than in other growth sectors. Arrows show tensile (↔) and compressive (≻≺) stresses on the sector zoning boundaries. c) Forces, **P**, created by compositional inhomogeneities perpendicular to the cross sectional plane that induce twisting. In gray growth sectors, lattice constant *a* is greater than in other growth sectors and (+) and (●) correspond to the compressive and tensile stresses, respectively.

This analysis of stress distribution has been mimicked with rubber pieces, sized and shaped as quartz growth sectors, which were stretched and compressed according to the distribution of lattice constants and glued together. The macroscopic crystal deformations were also simulated computationally by a course mechanical finite element method whereby forces imposed on subvolumes were allowed to reach a mechanical equilibrium through deformation. The twist sense and morphology were predicted correctly in both cases.[219,254] However, the estimated twist intensity turned out to be much smaller than that observed because of the plastic character of the deformation. Stress is resolved by dislocation ensembles, which not only induce twisting in this layer but also penetrate the new growing layers. Stress in the new growth layers drives multiplication of the defects enhancing the twisting. Penetration and multiplication of defects combined with stress relaxation by plastic deformation result in much stronger twist intensity than expected from the heterometry itself.

Similar analyses were applied to mica,[228–230] gypsum,[247,254] and oxalic acid dihydrate.[219,253,254] These substances all formed macroscopic crystals with well-developed growth sectors. Is the autodeformation mechanism applicable to tiny, fibrous crystallites? There is no direct evidence, but indirect support for extending the mechanism to other size domains includes:

1) Crystals of the same compound sometimes show similar twisting morphologies at very different scales. Quartz

forms not only macroscopic ($h > 1$ mm) twisted crystals but also thin ($h = 0.05$–1 μm[64]) twisted fibers in chalcedony spherulites. Potassium dichromate likewise forms large individual crystals[250] and twisted thin fibers in spherulites[6,205] and ($h = 0.4$ μm to 1 mm; Figure 3, 9b). Hippuric acid also forms individual twisted crystals ($h =$ 0.2–100 μm; Figure 1a,b) as well as twisted fibers in spherulties ($h = 0.2$–1 μm; Figure 1e).

2) Impurities are often a prerequisite for twisted crystals, large or small (Section 4.6).
3) Fibers show faceted morphologies, bases for the inhomogeneous impurity distribution over the cross section. The symmetry of the tip is in accord with morphological deformations (Section 4.3).

Twisting in resorcinol by autodeformation[11] was supported by computations of the enantioselective adsorption of tartaric acid derivatives on the mirror image facets, and for aspirin by calculations of strain induced by salicylic acid incorporation.[13]

Finally, the surface stress mechanism (Section 5.6) can be considered a variation of the autodeformation mechanism in which the surface layers differ in lattice constants from the crystal interior, not because of an impurity but because of intrinsic features of the surface structure.

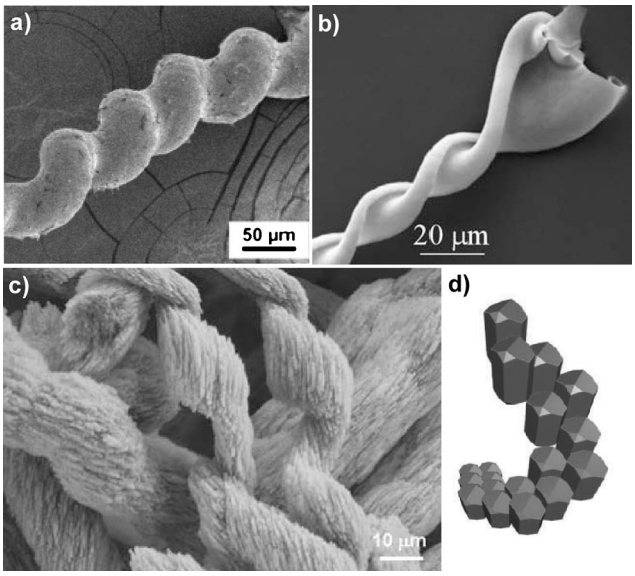

Figure 32. Helical polycrystalline aggregates. a) K_2SO_4 grown in the presence of poly(acrylic acid). Reproduced from Ref. [308] with permission. b) Silica/$BaCO_3$ biomorph. Reproduced from Ref. [342] with permission. c) $BaCO_3$ aggregate grown in the presence of polyethyleneglycol-*b*-[(2-[4-dihydroxyphosphoryl]-2-oxabutyl) acrylate ethyl ester] block copolymer. d) Schematic representation showing the orientation of crystallites in the aggregate shown in (c). Reproduced from Ref. [328] with permission.

6. Related Distortions

6.1. Polycrystalline and Amorphous Helices

Helical ensembles of crystals, introduced at the outset, are discovered with increasing frequency as chemists carry out crystallization from solutions containing all manner of complex macromolecular additives. Ball characterized such mixtures as "Shakespearean" when referring to earlier pioneers in the study of biomineralization.[323] Although curved polycrystalline and amorphous morphologies can grow from the vapor as for carbon,[215,324] silicon nitride,[215,325] silica,[326] and boron carbide,[327] most of these aggregates form in complex solutions, gels, and sols.

Imai and Oaki showed helical structures that result from a stacking of K_2SO_4 platelets in a polyacrylic acid solution (Figure 32a).[308] Coarsely textured $BaCO_3$, $BaSO_4$, and $BaCrO_4$ curved fibers and helices were prepared by Cölfen and co-workers by precipitation in the presence of a block copolymer (Figure 32c,d).[328–331] Curved $BaSO_4$ fibers were precipitated in the presence of surfactants.[332,333] Complex tetramethyl ammonium manganese oxides, such as $[N(CH_3)_4]^+_{0.93}Mn^{4+}_{2.1}Mn^{3+}_{1.9}O_7(OH)_{1.03}\cdot 5H_2O$, form polycrystalline helices when colloidal solutions confined in long, narrow tubes contract.[334,335]

Silica/carbonate biomorphs, $BaCO_3$, $SrCO_3$, or $CaCO_3$ composites obtained in co-precipitation with silica in a base, are among the most startling of laboratory-grown crystal forms.[336–347] As nanocrystalline carbonate salts precipitate, the pH value drops, depositing amorphous silica in turn that cements the crystalline phase. The fluctuations of pH value and coupled precipitations are oscillatory. This actualizes a twisting as shown in Figure 32b.[342] Biomorphs were most recently raised to an art form.[390] In these structures, the graceful curves are a collaboration between a nanocrystalline phase and an amorphous phase. The amorphous phases of biomorphs share some relation with amorphous calcium carbonate which is responsible for single-crystal biomineral forms with sculptured morphologies.[348] Silica itself can also crystallize as helical rods, nanotubes, and ribbons.[349–356] Morphogenesis seems to be related to the folding of planar structures as opposed to crystal growth. Generally speaking, biomorphs consist of numerous crystallites and amorphous particles with exotic shapes that do not arise from distortions of a lattice. They are distinct from the twisted crystals discussed above.

6.2. Nanotubes and Nanoscrolls

Curved morphologies are increasingly found at the nanoscale. They begin to form immediately after nucleation. Nanoscrolls, nanotubes, and fullerene-like morphologies formed of layered substances have been intensively studied during last 20 years. The best known example is carbon.[357–361] In addition to straight nanotubes, carbon also produces twisted nanotubes.[362–366] Metal chalcogenides (e.g. MoS_2, WS_2, ZnS, $Cu_{5.5}FeS_{6.5}$, $PbNb_nS_{2n+1}$), oxides (e.g. TiO_2, ZnO, Al_2O_3, V_2O_5, SiO_2, $NaSmF_4$, $BaTiO_3$, MoO_3), $NiCl_2$, BN, BCN, Si, metals (e.g. Au, Co, Fe, Te), $(C_4H_{12}N)_{14}[(UO_2)_{10}(SeO_4)_{14}(H_2O)]$ among many other substances[367–371] also form nanotubes. Nanotubes and nanoscrolls in oxide- and sulfide-based natural minerals (e.g. chrysotile $(Mg_3Si_2O_5(OH)_4)$,[372] cylin-

drite ($(Pb,Sn)_8Sb_4Fe_2Sn_5S_{27}$), imogolite ($Al_2SiO_3(OH)_4$), tochilinite ($6FeS{\cdot}5(Mg,Fe)(OH)_2$)) have been reviewed.[373] Analysis of curved morphologies involves consideration of the forces acting at the level of a single molecule or elementary layer but not on a 3D periodic crystal.

6.3. Transrotational Crystals

So-called transrotational crystals are a real puzzle to aficionados of unusual morphologies. These objects form in thin (< 100 nm) amorphous films and are thus flat. Nevertheless, lattices appear to rotate about the tangent axes that lie in the plane of the substrate and perpendicular to growth axis. In other words, crystallites 'roll' in the forward growth direction leading to periodic banded structures (Figure 33). This phenomenon was observed for Se,[288,374,375] Fe_2O_3,[374–376] and V_2O_3[377] fibers in spherulites, as well as for Cr_2O_3,[378] V_2O_3,[378] Ta_2O_5,[379] Ge-Te, Tl-Se, Cd-Te alloys,[380] and single crystals of Cu-Te alloys,[381] among others.[382] The growth mechanism responsible for such structures is not known.

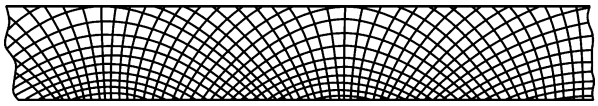

Figure 33. Scheme of bending of lattice planes (*hkl*) in a typical transrotational crystal. Reproduced from Ref. [380] with permission.

7. Summary and Outlook

Three-dimensional single crystals with curved lattice planes populate the crystallographic kingdom. Many of the distortions from long-range translational symmetry are actuated by growth.

Twisted and bent crystals range in size from $h = 5$ nm–3 cm. Our analysis shows that fields can sometimes induce crystal deformations but they most likely cannot yield well-organized helical morphologies. Periodic arrays of dislocations and twins are not a cause of a twisting moment, but rather a consequence. Other mechanisms discussed in Section 5 are initiated under the specific conditions and length scales illustrated in Figure 34.

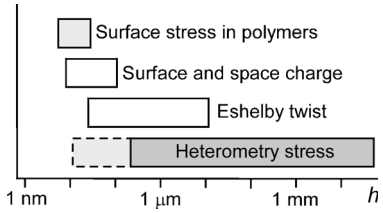

Figure 34. Correlation of deformation mechanism and minimum size, *h*, for twisted crystals. Unfilled rectangles indicate the absence of plastic relaxation; light-gray filling denotes partial plastic relaxation; darker gray denotes substantial plastic relaxation. It is unclear whether heterometry is important below 200 nm (dotted rectangle).

Genuine twisted crystals can be divided into two groups of crystals depending upon twisting mechanism. The first embraces objects with low dislocations densities and small sizes (*h* typically < 100 nm and rarely up to 10 μm). They may form curved morphologies through spontaneous polarization and piezoelastic phenomenon or stress on growth dislocations (Sections 5.1, 5.3). This group is small. The deformation is primarily elastic, since such micro- and nanoscale objects form at low temperatures from solution and the vapor. Twist intensity, purely physical in origin, does not depend directly on growth conditions and chemical environment.

The second group includes curved forms arising from crystal inhomogeneities and the corresponding stresses (Sections 5.6, 5.7). Stress is a unifying etiology in a majority of twisted crystals of all sizes. Stress begins to act through elastic distortions, but ultimately deformations are preserved plastically. This makes it difficult to assign a twisting mechanism from the degree of deformation (twist period, curvature radius) and the crystal size.

The driving force of deformation depends on the presence of specific impurities or on the structural state of the surface, assuming a strong control exerted by growth conditions and chemical composition. Chemical and structural inhomogeneity is a necessary, but not sufficient, condition for the twisting since the inhomogeneity-driven internal stress has to be able to create a twist moment. This can be achieved through the specific morphology and anatomy of a crystal that, in turn, is strongly controlled by the chemical environment and growth conditions.[219] Thus, in an ensemble of crystals grown under similar conditions from one and the same growth medium twist intensity can vary dramatically.

The weight of the evidence discussed herein encourages scientists to treat the association of a triplet of indices (*hkl*) with a plane as only an idealization, a mathematical fiction like the concept of the lattice itself. Helicoidal surfaces are normalized in Riemannian spaces.[383] So-called non-Euclidean crystallography requires disclinations.[384] Perhaps, this is a path to a fuller description of the details of the plastic distortions that are requisite in as-grown twisted crystals.

Already in 1907, Wallerant, the pioneer in the production of artificial growth-induced twisting of crystals, declared that the objects of his interest were the third class of anisotropic structure. "*To date we know of three kinds of anisotropic structures*", he said, "*crystalline bodies, Lehmann's anisotropic drops* [by this he meant liquid crystals], *and twisted crystals*".[75] In other words, Wallerant carved out a whole new category of matter on a par with crystals and liquid crystals. While this class of matter was admirably expanded by Bernauer,[1] it faded in its perceived significance, only to emerge again forcefully within the special context of high polymers.

The conspicuous absence of bent and twisted crystals from contemporary overviews of crystal growth and morphology may be another consequence[27,385,386] of the hegemony of X-ray crystallography in solid-state science during the past 100 years (exactly, at the time of submission, since the first crystal structures of the alkali halides by the Braggs in 1913[387,388]). Bent and twisted fibrils do not easily give up their atomic positions by X-ray scattering. They frequently occur in

polycrystalline films—especially organic molecular crystals—which chemists, focused on single-crystal structure determination, have been conditioned to ignore. However, the rise of area detectors prefigures a resurgence in the study of polycrystalline pattern formation of which crystal twisting and bending play no small part.

This project was supported by the US National Science Foundation (CHE-0845526, DMR-1105000) and by the Provost's Office of New York University.

Received: February 11, 2013

[1] F. Bernauer, *"Gedrillte" Kristalle*, Gebrüder Borntraeger, Berlin, **1929**.
[2] I. Sunagawa, *Crystals*: *Growth*, *Morphology*, *and Perfection*, Cambridge University Press, Cambridge, **2007**.
[3] I. V. Markov, *Crystal Growth for Beginners*: *Fundamentals of Nucleation*, *Crystal Growth and Epitaxy*, World Scientific, Singapur, **2004**.
[4] A. Pimpinelli, J. Villain, *Physics of Crystal Growth*, Cambridge University Press, Cambridge, **1999**.
[5] K. Jackson, *Kinetic Processes*, Wiley-VCH, Weinheim, **2010**.
[6] A. Shtukenberg, E. Gunn, M. Gazzano, J. Freudenthal, E. Camp, R. Sours, E. Rosseeva, B. Kahr, *ChemPhysChem* **2011**, *12*, 1558 – 1571.
[7] P. D. Calvert, D. R. Uhlmann, *J. Polym. Sci. Part B* **1973**, *11*, 457 – 465.
[8] A. G. Shtukenberg, J. Freudenthal, B. Kahr, *J. Am. Chem. Soc.* **2010**, *132*, 9341 – 9349.
[9] Hippuric acid single-crystalline fibers were grown by means of a physical evaporation condensation method ($T = 30$–$150\,^{\circ}C$) in the presence of the red impurity formed during high-temperature decomposition of hippuric acid.
[10] A. G. Shtukenberg, E. Gunn, L. Yu, B. Kahr, *Cryst. Growth Des.* **2011**, *11*, 4458 – 4462.
[11] B. Kahr, A. Shtukenberg, E. Gunn, D. J. Carter, A. L. Rohl, *Cryst. Growth Des.* **2011**, *11*, 2070 – 2073.
[12] A. G. Shtukenberg, Yu. O. Punin, E. Gunn, B. Kahr, *Chem. Rev.* **2012**, *112*, 1805 – 1838.
[13] X. Cui, A. Rohl, A. G. Shtukenberg, B. Kahr, *J. Am. Chem. Soc.* **2013**, *135*, 3395 – 3398.
[14] A. A. Chernov, *Modern Crystallography III*, *Crystal Growth*, Springer, Berlin, **1984**.
[15] R. W. Gurney, C. A. Mitchell, S. Ham, L. D. Bastin, B. Kahr, *J. Phys. Chem. B* **2000**, *104*, 878 – 892.
[16] H. E. Buckley, *Crystal growth*, Wiley, New York, **1951**.
[17] T. Lu, R. B. Yallee, C. K. Ong, I. Sunagawa, *J. Cryst. Growth* **1995**, *151*, 342 – 347.
[18] Yu. O. Punin, V. D. Franke, *Crystallogr. Rep.* **2004**, *49*, 310 – 314.
[19] L. J. Spencer, *Mineral. Mag.* **1921**, *19*, 263 – 274.
[20] D. P. Grigor'ev, *Ontogeny of Minerals*, Israel Program for Scientific Translations, Jerusalem, **1965**.
[21] L. Zhu, R. O. Al-Kaysi, Ch. J. Bardeen, *J. Am. Chem. Soc.* **2011**, *133*, 12569 – 12575.
[22] L. Zhu, R. O. Al-Kaysi, R. J. Dillon, F. S. Tham, C. J. Bardeen, *Cryst. Growth Des.* **2011**, *11*, 4975 – 4983.
[23] F. Terao, M. Morimoto, M. Irie, *Angew. Chem.* **2012**, *124*, 925 – 928; *Angew. Chem. Int. Ed.* **2012**, *51*, 901 – 904.
[24] S. Kobatake, S. Takami, H. Muto, T. Ishikawa, M. Irie, *Nature* **2007**, *446*, 778 – 781.
[25] M. Huang, U. Schilde, M. Kumke, M. Antonietti, H. Cölfen, *J. Am. Chem. Soc.* **2010**, *132*, 3700 – 3707.
[26] J. W. Cahn, R. E. Hanneman, *Surf. Sci.* **1964**, *1*, 387 – 398.
[27] A. G. Shtukenberg, Yu. O. Punin, *Optically Anomalous Crystals* (Ed.: B. Kahr), Springer, Dordrecht, **2007**.
[28] C. A. Knight, *J. Appl. Phys.* **1962**, *33*, 1808 – 1815.
[29] H. Cölfen, M. Antonietti, *Mesocrystals and Nonclassical Crystallization*, Wiley, New York, **2008**.
[30] H. Imai, Y. Oaki, *CrystEngComm* **2010**, *12*, 1679 – 1687.
[31] Y. Oaki, H. Imai, *Langmuir* **2007**, *23*, 5466 – 5470.
[32] H. Imai, Y. Oaki, *Angew. Chem.* **2004**, *116*, 1387 – 1392; *Angew. Chem. Int. Ed.* **2004**, *43*, 1363 – 1368.
[33] A. E. Rowan, R. J. M. Nolte, *Angew. Chem.* **1998**, *110*, 65 – 71; *Angew. Chem. Int. Ed.* **1998**, *37*, 63 – 68.
[34] E. Yashima, K. Maeda, H. Iida, Y. Furusho, K. Nagai, *Chem. Rev.* **2009**, *109*, 6102 – 6211.
[35] J. V. Selinger, M. S. Spector, J. M. Schnur, *J. Phys. Chem. B* **2001**, *105*, 7157 – 7169.
[36] L.-S. Li, H. Jiang, B. W. Messmore, S. R. Bull, S. I. Stupp, *Angew. Chem.* **2007**, *119*, 5977 – 5980; *Angew. Chem. Int. Ed.* **2007**, *46*, 5873 – 5876.
[37] A. Brizard, R. Oda, I. Huc, *Top. Curr. Chem.* **2005**, *256*, 167 – 218.
[38] *Topics in Stereochemistry*, Vol. 24 (Eds.: M. M. Green, R. J. M. Nolte, E. W. Meijer), Wiley-Interscience, New York, **2003**.
[39] *Chirality at the Nanoscale* (Ed.: D. B. Amabilino), Wiley-VCH, New York, **2009**.
[40] P. T. Lansbury, Jr., K. S. Kosik, *Chem. Biol.* **2000**, *7*, R9 – R12.
[41] B. Lotz, A. Gonthier-Vassal, A. Brack, J. Magoshi, *J. Mol. Biol.* **1982**, *156*, 345 – 357.
[42] J. O. Warwicker, *Acta Crystallogr.* **1954**, *7*, 565 – 573.
[43] K. Maeda, H. Mochizuki, K. Osato, E. Yashima, *Macromolecules* **2011**, *44*, 3217 – 3226.
[44] X. Wang, Y. Lu, Y. Duan, L. Meng, C. Li, *Adv. Mater.* **2008**, *20*, 462 – 465.
[45] W. E. Lindsell, P. N. Preston, J. M. Seddon, G. M. Rosair, T. A. J. Woodman, *Chem. Mater.* **2000**, *12*, 1572 – 1576.
[46] S. Chandrasekhar, *Liquid Crystals*, Cambridge University Press, Cambridge, **1993**.
[47] L. E. Hough, M. Spannuth, M. Nakata, D. A. Coleman, C. D. Jones, G. Dantlgraber, C. Tschierske, J. Watanabe, E. Körblova, D. M. Walba, J. E. Maclennan, M. A. Glaser, N. A. Clark, *Science* **2009**, *325*, 452 – 456.
[48] L. E. Hough, H. T. Jung, D. Krüerke, M. S. Heberling, M. Nakata, C. D. Jones, D. Chen, D. R. Link, J. Zasadzinski, G. Heppke, J. P. Rabe, W. Stocker, E. Körblova, D. M. Walba, M. A. Glaser, N. A. Clark, *Science* **2009**, *325*, 456 – 460.
[49] E. A. Matsumoto, G. P. Alexander, R. D. Kamien, *Phys. Rev. Lett.* **2009**, *103*, 257804.
[50] D. Chen, M.-S. Heberling, M. Nakata, L. E. Hough, J. E. Maclennan, M. A. Glaser, E. Korblova, D. M. Walba, J. Watanabe, N. A. Clark, *ChemPhysChem* **2012**, *13*, 155 – 159.
[51] D. Chen, J. E. Maclennan, R. Shao, D. K. Yoon, H. Wang, E. Korblova, D. M. Walba, M. A. Glaser, N. A. Clark, *J. Am. Chem. Soc.* **2011**, *133*, 12656 – 12663.
[52] T.-F. Lin, R.-M. Ho, C.-H. Sung, C.-S. Hsu, *Chem. Mater.* **2006**, *18*, 5510 – 5519.
[53] T. Gibaud, E. Barry, M. J. Zakhary, M. Henglin, A. Ward, Y. Yang, C. Berciu, R. Oldenbourg, M. F. Hagan, D. Nicastro, R. B. Meyer, Z. Dogic, *Nature* **2012**, *481*, 348 – 351.
[54] D. Krishnamurti, M. S. Madhava, D. Revannasiddaiah, *Mol. Cryst. Liq. Cryst.* **1978**, *47*, 155 – 177.
[55] D. Revannasiddaiah, M. S. Madhava, D. Krishnamurti, *Mol. Cryst. Liq. Cryst.* **1977**, *39*, 87 – 99.
[56] X. Xie, L. Ju, X. Feng, Y. Sun, R. Zhou, K. Liu, S. Fan, Q. Li, K. Jiang, *Nano Lett.* **2009**, *9*, 2565 – 2570.
[57] J. Sowerby, British Mineralogy, Vol. 4, Or, Coloured Figure Intended to Elucidate the Mineralogy of Great Britain A. R. Taylor and Company, London, **1811**.
[58] L. Bombicci, *Mem. Accad. Sci. Ist. Bologna* **1886**, *7*, 129.

[59] T. Wada (T. Gawa trans.) *Minerals of Japan*, Imperial University of Tokyo, Tokyo, **1904**, Plate VII, 2.
[60] O. Lehmann, *Molecularphysik*, Bd. 1, Verlag von Wilhelm Engelmann, Leipzig, **1888**.
[61] O. Breidbach, *Visions of Nature*: *The Art and Science of Ernst Haeckel*, Prestel, München, **2006**.
[62] E. Haeckel, *Kristallseelen – Studien über Inorganische Leben*, Alfren Kröner, Leipzig, **1917**; Trans. "Crystal Souls—Studies in Inorganic Life" A. Mackay, *Forma* **1999**, *14*, 1 – 204.
[63] A. Michel-Lévy, C. P. E. Munier-Chalmas, *Bull. Soc. Fr. Mineral.* **1892**, *15*, 159 – 190.
[64] N. M. Maleev, *Tschermaks Mineral. Petrogr. Mitt.* **1972**, *18*, 1 – 16.
[65] C. Frondel, *Am. Mineral.* **1978**, *63*, 17 – 27.
[66] Y. Wang, E. Merino, *Am. J. Sci.* **1995**, *295*, 49 – 77.
[67] E. Merino, Y. Wang, É. Deloule, *Am. J. Sci.* **1995**, *295*, 1156 – 1176.
[68] P. J. Heaney, A. M. Davis, *Science* **1995**, *269*, 1562 – 1565.
[69] J. Comer, P. Ortoleva, *Am. Mineral.* **2007**, *92*, 1952 – 1957.
[70] M. A. Lacroix, *C. R. Hebd. Seances Acad. Sci.* **1910**, *150*, 1388 – 1390.
[71] F. Wallerant, *Bull. Soc. Fr. Mineral.* **1897**, *20*, 52 – 100.
[72] L. Pasteur, *C. R. Hebd. Seances Acad. Sci.* **1848**, *26*, 535 – 539.
[73] F. Wallerant, *C. R. Hebd. Seances Acad. Sci.* **1906**, *143*, 553 – 557.
[74] F. Wallerant, *C. R. Hebd. Seances Acad. Sci.* **1906**, *143*, 1169 – 1170.
[75] F. Wallerant, *Bull. Soc. Fr. Mineral.* **1907**, *30*, 43 – 60.
[76] G. E. Bacon, E. J. Lisher, *Acta Crystallogr. Sect. B* **1980**, *36*, 1908 – 1916.
[77] P. Gaubert, *C. R. Hebd. Seances Acad. Sci.* **1908**, *146*, 829 – 831.
[78] P. Gaubert, *C. R. Hebd. Seances Acad. Sci.* **1913**, *156*, 1161 – 1163.
[79] P. Gaubert, *Bull. Soc. Fr. Mineral.* **1913**, *36*, 45 – 64.
[80] P. Gaubert, *C. R. Hebd. Seances Acad. Sci.* **1916**, *162*, 554 – 556.
[81] P. Gaubert, *Bull. Soc. Fr. Mineral.* **1911**, *32*, 422 – 437.
[82] P. Gaubert, *C. R. Hebd. Seances Acad. Sci.* **1911**, *153*, 683 – 685.
[83] P. Gaubert, *Ann. Chim.* **1916**, *5 – 6*, 356 – 364.
[84] P. Gaubert, *C. R. Hebd. Seances Acad. Sci.* **1917**, *164*, 355 – 357.
[85] P. Gaubert, *Bull. Soc. Fr. Mineral.* **1918**, *41*, 198 – 224.
[86] P. Gaubert, *Bull. Soc. Fr. Mineral.* **1918**, *167*, 368 – 370.
[87] P. Gaubert, *Bull. Soc. Fr. Mineral.* **1922**, *175*, 973 – 975.
[88] P. Gaubert, *Bull. Soc. Fr. Mineral.* **1925**, *80*, 1853 – 1855.
[89] P. Gaubert, *Festschrift Victor Goldschmidt*, Carl Winters Universitätsbuchhandlung, Heidelberg, **1928**, pp. 98 – 107.
[90] P. Gaubert, *C. R. Hebd. Seances Acad. Sci.* **1931**, *92*, 1576 – 1579.
[91] A. V. Shubnikov, V. A. Kopstik, *Symmetry in Art and Science*, Plenum, New York, **1974**.
[92] A. V. Shubnikov, *Sov. Phys. Crystallogr.* **1956**, *1*, 500 – 502.
[93] J. J. Point, *Bull. Cl. Sci. Acad. R. Belg.* **1953**, *39*, 455.
[94] J. J. Point, *Bull. Cl. Sci. Acad. R. Belg.* **1955**, *41*, 982.
[95] H. D. Keith, F. J. Padden, *J. Polym. Sci.* **1959**, *39*, 123 – 138.
[96] H. D. Keith, F. J. Padden, *J. Polym. Sci.* **1958**, *31*, 415 – 421.
[97] A. Keller, *J. Polym. Sci.* **1959**, *39*, 151 – 173.
[98] F. P. Price, *J. Polym. Sci.* **1959**, *39*, 139 – 150.
[99] B. Lotz, S. Z. D. Cheng, *Polymer* **2005**, *46*, 577 – 610.
[100] A. Keller, *Nature* **1952**, *169*, 913 – 914.
[101] N. H. Hartshorne, *Nature* **1961**, *190*, 1191 – 1192.
[102] B. Popoff, *Latv. Farm. Zurn.* **1934**, 1.
[103] L. Yu, *J. Am. Chem. Soc.* **2003**, *125*, 6380 – 6381.
[104] J. Tao, L. Yu, *J. Phys. Chem. B* **2006**, *110*, 7098 – 7101.
[105] A. G. Shtukenberg, X. Cui, J. Freudenthal, E. Gunn, E. Camp, B. Kahr, *J. Am. Chem. Soc.* **2012**, *134*, 6354 – 6364.
[106] J. L. Hutter, J. Bechhoefer, *Phys. Rev. Lett.* **1997**, *79*, 4022 – 4025.
[107] J. L. Hutter, J. Bechhoefer, *Phys. Rev. E* **1999**, *59*, 4342 – 4352.
[108] J. L. Hutter, J. Bechhoefer, *J. Cryst. Growth* **2000**, *217*, 332 – 343.
[109] W. Pisula, M. Kastler, D. Wasserfallen, T. Pakula, K. Müllen, *J. Am. Chem. Soc.* **2004**, *126*, 8074 – 8075.
[110] N. Z. Evzikova in *The Genesis of Mineral Individuals and Aggregates*, Nauka, Moskau, **1966**, pp. 234 – 244 (in Russian).
[111] R. Bacon, *J. Appl. Phys.* **1960**, *31*, 283 – 290.
[112] D. D. Double, A. Hellawell, *Acta Metall.* **1974**, *22*, 481 – 487.
[113] B. Miao, D. O. N. Wood, W. Bian, K. Fang, M. H. Fan, *J. Mater. Sci.* **1994**, *29*, 255 – 261.
[114] K. He, H. R. Daniels, A. Brown, R. Brydson, D. V. Edmonds, *Acta Mater.* **2007**, *55*, 2919 – 2927.
[115] M. I. Kozlovskii, *Sov. Phys. Crystallogr.* **1965**, *10*, 101 – 103.
[116] G. Ryschenkow, G. Faivre, *J. Cryst. Growth* **1988**, *87*, 221 – 235.
[117] J. Bisault, G. Ryschenkow, G. Faivre, *J. Cryst. Growth* **1991**, *110*, 889 – 909.
[118] G. Shuur, *J. Polym. Sci.* **1961**, *50*, 191 – 209.
[119] D. C. Bassett, R. H. Olley, S. J. Sutton, A. S. Vaughan, *Macromolecules* **1996**, *29*, 1852 – 1853.
[120] J. Xu, B.-H. Guo, J.-J. Zhou, L. Li, J. Wu, M. Kowalczuk, *Polymer* **2005**, *46*, 9176 – 9185.
[121] A. Keller, *J. Polymer Sci.* **1955**, *17*, 291 – 308.
[122] D. C. Bassett, *Polymer* **2006**, *47*, 3263 – 3266.
[123] J. J. Janimak, L. Markey, G. C. Stevens, *Polymer* **2001**, *42*, 4675 – 4685.
[124] A. Toda, M. Okamura, K. Taguchi, M. Hikosaka, H. Kajioka, *Macromolecules* **2008**, *41*, 2484 – 2493.
[125] A. Toda, K. Taguchi, H. Kajioka, *Macromolecules* **2008**, *41*, 7505 – 7512.
[126] M. Rosenthal, D. V. Anokhin, V. A. Luchnikov, R. J. Davies, C. Riekel, M. Burghammer, G. Bar, D. I. Ivanov, *IOP Conf. Ser.: Mater. Sci. Eng.* **2010**, *14*, 012014.
[127] M. Rosenthal, G. Bar, M. Burghammer, D. I. Ivanov, *Angew. Chem.* **2011**, *123*, 9043 – 9047; *Angew. Chem. Int. Ed.* **2011**, *50*, 8881 – 8885.
[128] D. C. Bassett, A. M. Hodge, *Proc. R. Soc. London Ser. A* **1981**, *377*, 61 – 71.
[129] H. D. Keith, F. J. Padden, Jr., *Polymer* **1984**, *25*, 28 – 42.
[130] A. Lustiger, B. Lotz, T. S. Duff, *J. Polym. Sci. Part B* **1989**, *27*, 561 – 579.
[131] A. Keller, *Macromol. Chem.* **1959**, *34*, 1 – 28.
[132] M. I. Abo el Maaty, D. C. Bassett, *Polymer* **2002**, *43*, 6541 – 6549.
[133] H. D. Keith, F. J. Padden, Jr., *Macromolecules* **1996**, *29*, 7776 – 7786.
[134] D. Maillard, R. E. Prud'homme, *Macromolecules* **2008**, *41*, 1705 – 1712.
[135] J. Foks, M. Łusczczek, *J. Cryst. Growth* **1993**, *134*, 347 – 352.
[136] E. M. Woo, J.-H. Lin, *Polymer* **2006**, *47*, 6826 – 6835.
[137] E. M. Woo, Y.-F. Chen, *Polymer* **2009**, *50*, 4706 – 4717.
[138] A. J. Owen, *Polymer* **1997**, *38*, 3705 – 3708.
[139] M. Imai, K. Kaji, *Polymer* **2006**, *47*, 5544 – 5554.
[140] T. Wang, H. Wang, H. Li, Z. Gan, S. Yan, *Phys. Chem. Chem. Phys.* **2009**, *11*, 1619 – 1627.
[141] Y. Okabe, T. Kyu, H. Saito, T. Inoue, *Macromolecules* **1998**, *31*, 5823 – 5829.
[142] P. Hong, W.-T. Chung, C.-F. Hsu, *Polymer* **2002**, *43*, 3335 – 3343.
[143] T. Ikehara, H. Jinnai, T. Kaneko, H. Nishioka, T. Nishi, *J. Polym. Sci. Part B* **2007**, *45*, 1122 – 1125.
[144] Y. Nozue, R. Kurita, S. Hirano, N. Kawasaki, S. Ueno, A. Iida, T. Nishi, Y. Amemiya, *Polymer* **2003**, *44*, 6397 – 6405.
[145] Y. Nozue, S. Hirano, R. Kurita, N. Kawasaki, S. Ueno, A. Iida, T. Nishi, Y. Amemiya, *Polymer* **2004**, *45*, 8299 – 8302.
[146] H. Tanaka, T. Ikeda, T. Nishi, *Appl. Phys. Lett.* **1986**, *48*, 393 – 395.
[147] J. Liu, F. Zhang, T. He, *Macromol. Rapid Commun.* **2001**, *22*, 1340 – 1343.

[148] P. J. Barham, A. Keller, E. L. Otun, P. A. Holmes, *J. Mater. Sci.* **1984**, *19*, 2781 – 2794.
[149] K. L. Singfield, J. K. Hobbs, A. Keller, *J. Cryst. Growth* **1998**, *183*, 683 – 689.
[150] J. K. Hobbs, D. R. Binger, A. Keller, P. J. Barham, *J. Polym. Sci. Part B* **2000**, *38*, 1575 – 1583.
[151] Q. K. Cao, X. P. Qiao, H. Wang, J. P. Liu, *Sci. China Ser. B* **2008**, *51*, 853 – 858.
[152] H.-M. Ye, J.-S. Wang, S. Tang, J. Xu, X.-Q. Feng, B.-H. Guo, X.-M. Xie, J.-J. Zhou, L. Li, Q. Wu, G.-Q. Chen, *Macromolecules* **2010**, *43*, 5762 – 5770.
[153] M. Gazzano, M. L. Focarete, C. Riekel, M. Scandola, *Biomacromolecules* **2000**, *1*, 604 – 608.
[154] M. Gazzano, M. L. Focarete, C. Riekel, A. Ripamonti, M. Scandola, *Macromol. Chem. Phys.* **2001**, *202*, 1405 – 1409.
[155] T. Tanaka, M. Fujita, A. Takeuchi, Y. Suzuki, K. Uesugi, Y. Doi, T. Iwata, *Polymer* **2005**, *46*, 5673 – 5679.
[156] H. D. Keith, F. J. Padden, Jr., T. P. Russell, *Macromolecules* **1989**, *22*, 666 – 675.
[157] J. H. Magill, *J. Mater. Sci.* **2001**, *36*, 3143 – 3164.
[158] See Ref. [120].
[159] M. Gazzano, M. L. Focarete, C. Riekel, M. Scandola, *Biomacromolecules* **2004**, *5*, 553 – 558.
[160] D. Maillard, R. E. Prud'homme, *Macromolecules* **2006**, *39*, 4272 – 4275.
[161] I. Saracovan, H. D. Keith, R. St. J. Manley, G. R. Brown, *Macromolecules* **1999**, *32*, 8918 – 8922.
[162] K. L. Singfield, G. R. Brown, *Macromolecules* **1995**, *28*, 1290 – 1297.
[163] K. L. Singfield, J. M. Klass, G. R. Brown, *Macromolecules* **1995**, *28*, 8006 – 8015.
[164] A. Toda, T. Arita, M. Hikosaka, *Polymer* **2001**, *42*, 2223 – 2233.
[165] A. Toda, T. Arita, M. Hikosaka, J. K. Hobbs, M. J. Miles, *J. Macromol. Sci. Part B* **2003**, *42*, 753 – 760.
[166] A. Toda, K. Taguchi, M. Hikosaka, H. Kajioka, *Polym. J.* **2008**, *40*, 905 – 909.
[167] A. S. Vaughan, *J. Mater. Sci.* **1993**, *28*, 1805 – 1813.
[168] B. Lotz, A. Thierry, *Macromolecules* **2003**, *36*, 286 – 290.
[169] C.-C. Chao, C.-K. Chen, Y. W. Chiang, R.-M. Ho, *Macromolecules* **2008**, *41*, 3949 – 3956.
[170] M. Kunz, M. Drechsler, M. Möller, *Polymer* **1995**, *36*, 1331 – 1339.
[171] C. Y. Li, D. Yan, S. Z. D. Cheng, F. Bai, T. He, L.-C. Chien, F. W. Harris, B. Lotz, *Macromolecules* **1999**, *32*, 524 – 527.
[172] J. Wang, C. Y. Li, S. Jin, X. Weng, R. M. Van Horn, M. J. Graham, W.-B. Zhang, K.-U. Zheong, F. W. Harris, B. Lotz, S. Z. D. Cheng, *Ind. Eng. Chem. Res.* **2010**, *49*, 11936 – 11947.
[173] W. Cai, C. Y. Li, L. Li, B. Lotz, M. Keating, D. Marks, *Adv. Mater.* **2004**, *16*, 600 – 605.
[174] T. E. Wellems, R. Josephs, *J. Mol. Biol.* **1980**, *137*, 443 – 450.
[175] H. M. White, I. L. Hosier, D. C. Bassett, *Macromolecules* **2002**, *35*, 6763 – 6765.
[176] A. L. McClellan, *J. Chem. Phys.* **1960**, *32*, 1271 – 1272.
[177] T. Tachibana, H. Kambara, *J. Am. Chem. Soc.* **1965**, *87*, 3015 – 3016.
[178] M. J. Bierman, Y. K. A. Lau, A. V. Kvit, A. L. Schmitt, S. Jin, *Science* **2008**, *320*, 1060 – 1063.
[179] J. Zhu, H. Peng, A. F. Marshall, D. M. Barnett, W. D. Nix, Y. Cui, *Nat. Nanotechnol.* **2008**, *3*, 477 – 481.
[180] H.-F. Zhang, C.-M. Wang, L.-S. L. Wang, *Nano Lett.* **2002**, *2*, 941 – 944.
[181] G. W. Sears, *J. Chem. Phys.* **1959**, *31*, 53 – 54.
[182] B. Jeszenszky, E. Hartmann, *Nature* **1961**, *189*, 213.
[183] Yu. O. Punin, T. P. Ulyanova, T. G. Petrov, *Crystallography and Crystal Chemistry*, *N 2*, Leningrad Univ. Press, Leningrad, **1973**, pp. 97 – 100 (in Russian).
[184] M. Yang, N. A. Kotov, *J. Mater. Chem.* **2011**, *21*, 6775 – 6792.
[185] X. Y. Kong, Z. L. Wang, *Nano Lett.* **2003**, *3*, 1625 – 1631.
[186] X. Y. Kong, Z. L. Wang, *Appl. Phys. Lett.* **2004**, *84*, 975 – 977.
[187] X. Y. Kong, Y. Ding, R. Yang, Z. L. Wang, *Science* **2004**, *303*, 1348 – 1351.
[188] W. L. Hughes, Z. L. Wang, *J. Am. Chem. Soc.* **2004**, *126*, 6703 – 6709.
[189] P. X. Gao, W. Mai, Z. L. Wang, *Nano Lett.* **2006**, *6*, 2536 – 2543.
[190] Z. C. Tu, Q. X. Li, X. Hu, *Phys. Rev. B* **2006**, *73*, 115402.
[191] C. Majidi, Z. Chen, D. J. Srolovitz, M. Haataja, *J. Mech. Phys. Solids* **2010**, *58*, 73 – 85.
[192] Z. L. Wang, *J. Phys. Condens. Matter* **2004**, *16*, R829 – R858.
[193] J. K. Jian, Z. H. Zhang, Y. P. Sun, M. Lei, X. L. Chen, T. M. Wang, C. Wang, *J. Cryst. Growth* **2007**, *303*, 427 – 432.
[194] J. Duan, S. Yang, H. Liu, J. Gong, H. Huang, X. Zhao, J. Tang, R. Zhang, Y. Du, *J. Cryst. Growth* **2005**, *283*, 291 – 296.
[195] G. Z. Shen, Y. Bando, C. Y. Zhi, X. L. Yuan, T. Sekiguchi, D. Golberg, *Appl. Phys. Lett.* **2006**, *88*, 243106.
[196] G. Shen, D. Chen, *J. Am. Chem. Soc.* **2006**, *128*, 11762 – 11763.
[197] R. Yang, Z. L. Wang, *J. Am. Chem. Soc.* **2006**, *128*, 1466 – 1467.
[198] K. Kawabata, T. Kumagai, M. Mizutani, T. Sambongi, *J. Phys. I* **1996**, *6*, 1575 – 1580.
[199] D. M. Ho, R. A. Pascal, Jr., *Chem. Mater.* **1993**, *5*, 1358 – 1361.
[200] J. M. Blatchly, N. H. Hartshorne, *Trans. Faraday Soc.* **1966**, *62*, 512 – 518.
[201] Small (several microns thick) twisted crystals of resorcinol were grown over boiling resorcinol solution in benzene containing L- or D-tartaric acid.
[202] Y. Oaki, H. Imai, *Cryst. Growth Des.* **2003**, *3*, 711 – 716.
[203] H. Imai, Y. Oaki, A. Kotachi, *Bull. Chem. Soc. Jpn.* **2006**, *79*, 1834 – 1851.
[204] Y. Oaki, H. Imai, *Trans. Mater. Res. Soc. Jpn.* **2005**, *30*, 353 – 356.
[205] Y. Oaki, H. Imai, *J. Am. Chem. Soc.* **2004**, *126*, 9271 – 9275.
[206] R. G. Treuting, *Acta Metall.* **1957**, *5*, 173 – 175.
[207] E. F. Riebling, W. W. Webb, *Science* **1957**, *126*, 309.
[208] W. W. Webb, R. D. Dragsdorf, W. D. Forgeng, *Phys. Rev.* **1957**, *108*, 498 – 499.
[209] W. W. Webb, W. D. Forgeng, *J. Appl. Phys.* **1957**, *28*, 1449 – 1454.
[210] R. D. Dragsdorf, W. W. Webb, *J. Appl. Phys.* **1958**, *29*, 817 – 819.
[211] S. Mardix, A. R. Lang, G. Kowalski, A. P. W. Makepeace, *Philos. Mag. A* **1987**, *56*, 251 – 261.
[212] D. D. Double, P. Truelove, A. Hellawell, *J. Cryst. Growth* **1968**, *2*, 191 – 198.
[213] T. Attallah, J. E. Gruzleski, *J. Cryst. Growth* **1976**, *34*, 164 – 172.
[214] D. P. Mourer, J. D. Verhoeven, *J. Cryst. Growth* **1977**, *37*, 197 – 203.
[215] S. Motojima, *J. Ceram. Soc. Jpn.* **2008**, *116*, 921 – 927.
[216] S. Motojima, Y. Takahashi, K. Sugiyama, *J. Cryst. Growth* **1976**, *33*, 116 – 124.
[217] M. N. Maleev, *Properties and Genesis of Natural Thread-like Crystals and Aggregates*, Nauka, Moskau, **1971** (in Russian).
[218] E. M. Spiridonov, T. T. Abramova, L. L. Panas'yan, V. N. Sokolov, M. S. Chernov, O. I. Gusarova, V. M. Ladygin, *Dokl. Earth Sci.* **2008**, *421A*, 1000 – 1003.
[219] Yu. O. Punin, A. G. Shtukenberg, *Autodeformation Defects in Crystals*, St. Petersburg Univ. Press, St. Petersburg, **2008** (in Russian).
[220] M. Žorž, *Geologija* **1993**, *36*, 211 – 222.
[221] C. Frondel, *Amer. Mus. Novit.* **1936**, *N829*, 1 – 5.
[222] M. A. Kuz'mina, Yu. O. Punin, I. E. Kamentsev, *Zap. Vses. Mineral. O-va.* **1987**, *116*, N4, 445 – 453 (in Russian).
[223] G. G. Laemmlein, *Dokl. Akad. Nauk SSSR* **1936**, *4*, N6, 269 – 272 (in Russian).
[224] G. G. Laemmlein, *Izv. Akad. Nauk SSSR* **1937**, *5*, 937 – 964 (in Russian).
[225] P. P. Yukhtanov, *Twisted Crystals of Quartz*, Komi Nauch. Center. Akad Nauk SSSR Press, Syktyvkar **1989** (in Russian).

[226] R. Brauns, *The Mineral Kingdom*, (Ed.: L. J. Spencer), Lippincott, Philadelphia, **1912**.
[227] G. Tschermak, *Akad. Wiss. Wien* **1894**, *61*, 365 – 400.
[228] A. G. Shtukenberg, Yu. O. Punin, E. N. Kotelnikova, *Zap. Vseross. Mineral. O-va.* **1993**, *122*, N5, 53 – 63 (in Russian).
[229] Yu. O. Punin, E. N. Kotelnikova, Yu. E. Makagonova, P. B. Sokolov, *Zap. Vseross. Mineral. O-va* **1997**, *126*, N2, 23 – 36 (in Russian).
[230] P. B. Sokolov, Yu. O. Punin, E. N. Kotelnikova, Yu. L. Krezer, N. N. Predtechenskii, *Mineral. Zh.* **1987**, *9*, N1, 55 – 63 (in Russian).
[231] S. A. Borodin, *Zap. Vses. Mineral. O-va* **1961**, *90*, 578 – 586 (in Russian).
[232] J. M. Dymkov, V. A. Slyotov, V. N. Filippov, *New data on minerals*, Vol. 39 (Ed.: M. I. Novgorodova), Ocean Pictures, Moskau, **2004**, pp. 113 – 118.
[233] H. A. Miers, *Mineralogy*: *An Introduction to the Scientific Study of Minerals*, MacMillan, London, **1902**.
[234] B. M. Radke, R. L. Mathis, *J. Sediment. Petrol.* **1980**, *50*, 1149 – 1168.
[235] J. M. Gregg, *J. Sediment. Petrol.* **1983**, *53*, 1025 – 1033.
[236] A. Searl, *Mineral. Mag.* **1989**, *53*, 547 – 555.
[237] M. S. Pichugin, Yu. A. Kharitonov, N. V. Belov, *Zap. Vses. Mineral. O-va* **1969**, *98*, 55 – 58 (in Russian).
[238] D. J. Barber, R. J. Reeder, D. J. Smith, *Contrib. Mineral. Petrol.* **1985**, *91*, 82 – 92.
[239] V. B. Tatarsky, *Zap. Vses. Mineral. O-va.* **1935**, *64*, N1, 207 – 214 (in Russian).
[240] G. Yu. Boyarko, *Mineral. Zh.* **1983**, *5*, 57 – 63 (in Russian).
[241] The collection of the crystallography department, of St. Petersburg State University, Russia, contains a sample with molybdenite scrolls (up to 2 mm in diameter and 5 mm in length) from Ural mountains.
[242] A. C. Hawkins, *Am. Mineral.* **1933**, *18*, 274 – 275.
[243] V. G. Feklichev, *Microcrystallomorphological Analysis*, Moskau, Nauka, **1966** (in Russian).
[244] C. Rinaudo, M. Franchini-Angela, R. Boistelle, *J. Cryst. Growth* **1988**, *89*, 257 – 266.
[245] C. Rinaudo, M. Franchini-Angela, R. Boistelle, *Mineral. Mag.* **1989**, *53*, 479 – 482.
[246] Yu. O. Punin, O. I. Artamonova, *Zap. Vseross. Mineral. O-va.* **2000**, *129*, 90 – 94 (in Russian).
[247] Yu. O. Punin, O. I. Artamonova, *Crystallogr. Rep.* **2001**, *46*, 138 – 143.
[248] J. Suda, M. Matsushita, *J. Phys. Soc. Jpn.* **1995**, *64*, 348 – 351.
[249] J. Suda, T. Nakayama, A. Nakahara, M. Matsushita, *J. Phys. Soc. Jpn.* **1996**, *65*, 771 – 777.
[250] J. Suda, M. Matsushita, K. Izumi, *J. Phys. Soc. Jpn.* **2000**, *69*, 124 – 129.
[251] J. Suda, T. Nakayama, M. Matsushita, *J. Phys. Soc. Jpn.* **1998**, *67*, 2981 – 2983.
[252] J. Suda, M. Matsushita, *J. Phys. Soc. Jpn.* **2004**, *73*, 300 – 302.
[253] Y. O. Punin, O. M. Boldyreva, *Physics of Crystallization*, Kalinin Univ. Press, Kalinin, **1980**, pp. 46 – 55 (in Russian).
[254] M. A. Kuz'mina, S. V. Moshkin, Y. O. Punin, *Physics of Crystallization*, Tver University Press, Tver, **1991**, pp. 24 – 35 (in Russian).
[255] Oxalic acid dihydrate single crystals were grown at room temperature from acetic acid and acetone. The concentration of the solvent in the crystals grown was determined by ^{1}H NMR.
[256] M. Žorž, *Mineralien Welt* **2009**, *20*, 30 – 46.
[257] Z. Chen, C. Majidi, D. J. Srolovitz, M. Haataja, *Appl. Phys. Lett.* **2011**, *98*, 011906.
[258] R. Oda, I. Huc, M. Schmutz, S. J. Candau, F. C. MacKintosh, *Nature* **1999**, *399*, 566 – 569.
[259] C. Y. Li, S. Z. D. Cheng, J. J. Ge, F. Bai, J. Z. Zhang, I. K. Mann, F. W. Harris, L.-C. Chien, D. Yan, T. He, B. Lotz, *Phys. Rev. Lett.* **1999**, *83*, 4558 – 4561.
[260] D. Patel, D. C. Bassett, *Polymer* **2002**, *43*, 3795 – 3802.
[261] Y. Duan, Y. Jiang, S. Jiang, L. Li, S. Yan, J. M. Schultz, *Macromolecules* **2004**, *37*, 9283 – 9286.
[262] J. Xu, B.-H. Guo, G.-Q. Chen, Z.-M. Zhang, *J. Polym. Sci. Part B* **2003**, *41*, 2128 – 2134.
[263] K. Iwamoto, S.-I. Mitomo, M. Seno, *J. Colloid Interface Sci.* **1984**, *102*, 477 – 482.
[264] J. F. J. Dippy, *J. Phys. Chem.* **1932**, *36*, 2354 – 2361.
[265] E. S. Hedges, *Liesegang Rings and Other Periodic Structures*, Chapman & Hall, London, **1932**.
[266] H. D. Keith, F. J. Padden, *J. Polym. Sci.* **1959**, *39*, 101 – 122.
[267] H.-M. Ye, J. Xu, B.-H. Guo, T. Iwata, *Macromolecules* **2009**, *42*, 694 – 701.
[268] R. Oldenbourg, G. Mei, *J. Microsc.* **1995**, *180*, 140 – 147.
[269] E. Gunn, R. Sours, J. B. Benedict, W. Kaminsky, B. Kahr, *J. Am. Chem. Soc.* **2006**, *128*, 14234 – 14235.
[270] F. N. Bernauer, *Neues Jahrb. Mineral. Geol. Palaeontol. Abh. Abt.* **1927**, *55*, 92 – 143.
[271] J. J. Point, *Polymer* **2006**, *47*, 3186 – 3196.
[272] L. B. Morgan, *J. Appl. Chem.* **1954**, *4*, 160 – 172.
[273] L. B. Morgan, *Polymer* **1968**, *9*, 375 – 397.
[274] D. C. Bassett, *J. Macromol. Sci. B* **2003**, *42*, 227 – 256.
[275] A. W. Thornton, P. Predecki, *J. Appl. Phys.* **1970**, *41*, 4266 – 4273.
[276] J. Xu, B.-H. Guo, Z.-M. Zhang, J.-J. Zhou, Y. Jiang, S. Yan, L. Li, Q. Wu, G.-Q. Chen, J. M. Schultz, *Macromolecules* **2004**, *37*, 4118 – 4123.
[277] C. Y. Li, S. Z. D. Cheng, J. J. Ge, F. Bai, J. Z. Zhang, I. K. Mann, L.-C. Chien, F. W. Harris, B. Lotz, *J. Am. Chem. Soc.* **2000**, *122*, 72 – 79.
[278] T. Sugawara, Y. Suwa, K. Ohkawa, H. Yamamoto, *Macromol. Rapid Commun.* **2003**, *24*, 847 – 851.
[279] S. Hayashi, K. Ohkawa, Y. Suwa, T. Sugawara, T. Asami, H. Yamamoto, *Macromol. Biosci.* **2008**, *8*, 46 – 59.
[280] F. Glaab, M. Kellermeier, W. Kunz, *Macromol. Rapid Commun.* **2007**, *28*, 1024 – 1028.
[281] S. Timoshenko, J. N. Goodier, *Theory of Elasticity*, McGraw Hill, Singapur, **1982**.
[282] L. Lin, A. S. Argon, *J. Mater. Sci.* **1994**, *29*, 294 – 323.
[283] J. P. Poirier, *Creep of Crystals*: *High Temperature Deformation Processes in Metals*, Ceramics and Minerals, Cambridge Univ. Press, Cambridge, **1985**.
[284] L. A. Shuvalov, *Modern Crystallography IV*, *Physical Properties of Crystals*, Springer, Berlin, **1988**.
[285] R. W. K. Honeycombe, *The Plastic Deformation of Metals*, 2nd ed., Edward Arnold, London, **1984**.
[286] H. J. Frost, M. F. Ashby, *Deformation-Mechanism Maps*: *The Plasticity and Creep of Metals and Ceramics*, Pergamon, Oxford, **1982**.
[287] V. L. Indenbom, V. B. Osvenskii, *Growth of Crystals*, Vol. 13 (Ed.: E. I. Givargizov), Consultants Bureau, New York, **1980**, p. 279.
[288] I. E. Bolotov, V. Yu. Kolosov, A. V. Kozhyn, *Phys. Status Solidi A* **1982**, *72*, 645 – 654.
[289] V. I. Vladimirov, A. E. Romanov, *Disclinations in Crystals*, Nauka, Leningrad, **1986** (in Russian).
[290] A. E. Romanov, V. I. Vladimirov, *Dislocations in Crystals*, Vol. 9, Elsevier, Amsterdam, **1992**, pp. 191 – 402.
[291] C. A. Pampillo, L. A. Davis, *J. Appl. Phys.* **1972**, *43*, 4277 – 4285.
[292] *Springer Handbook of Condensed Matter and Materials Data*, *XVII* (Eds.: W. Martienssen, H. Warlimont), Springer, **2005**, pp. 477 – 522.
[293] Z. Wang, Y. Li, J. Yang, Q. Gou, Y. Wu, X. Wu, P. Liu, Q. Gu, *Macromolecules* **2010**, *43*, 4441 – 4444.

[294] C. Kübel, L. González-Ronda, L. F. Drummy, D. C. Martin, *J. Phys. Org. Chem.* **2000**, *13*, 816 – 829.
[295] L. González-Ronda, D. C. Martin, *Macromolecules* **1997**, *30*, 1524 – 1526.
[296] S. S. Sheiko, M. Gerle, K. Fischer, M. Schmidt, M. Möller, *Langmuir* **1997**, *13*, 5368 – 5372.
[297] L. Ziserman, A. Mor, D. Harries, D. Danino, *Phys. Rev. Lett.* **2011**, *106*, 238105.
[298] J. Comer, P. Ortoleva, *Am. Mineral.* **2007**, *92*, 1952 – 1957.
[299] M. P. Shaskol'skaya, P. P. Pashkov, *Sov. Phys. Crystallogr.* **1961**, *6*, 381 – 383.
[300] N. M. Beljaev, *Strength of Materials*, Nauka, Moskau, **1965** (in Russian).
[301] J. M. Schultz, D. R. Kinloch, *Polymer* **1969**, *10*, 271 – 278.
[302] H. D. Keith, W. Y. Chen, *Polymer* **2002**, *43*, 6263 – 6272.
[303] D. C. Bassett, *Philos. Trans. R. Soc. London Ser. A* **1994**, *348*, 29 – 43.
[304] J. D. Eshelby, *J. Appl. Phys.* **1953**, *24*, 176 – 179.
[305] J. D. Eshelby, *Philos. Mag.* **1958**, *3*, 440 – 447.
[306] D. R. Veblen, J. E. Post, *Am. Mineral.* **1983**, *68*, 790 – 803.
[307] R. Gomer, *J. Chem. Phys.* **1958**, *28*, 457 – 464.
[308] Y. Oaki, H. Imai, *Langmuir* **2005**, *21*, 863 – 869.
[309] S. Ibe, R. Ise, Y. Oaki, H. Imai, *CrystEngComm* **2012**, *14*, 7444 – 7449.
[310] R. Ise, Y. Oaki, H. Imai, *Cryst. Growth Des.* **2012**, *12*, 4397 – 4402.
[311] O. G. Kozlova, N. V. Belov, *Sov. Phys. Dokl.* **1981**, *26*, 805.
[312] X. Hu, P. R. Buseck, G. Luo, *Am. Mineral.* **1998**, *83*, 542 – 545.
[313] J. M. Schultz, *Polymer* **2003**, *44*, 433 – 441.
[314] M. Raimo, *J. Mater. Sci.* **2007**, *42*, 998 – 1003.
[315] V. S. Yoffe, *Usp. Khim.* **1944**, *13*, 144 – 161.
[316] J.-S. Wang, X.-Q. Feng, G.-F. Wang, S.-W. Yu, *Appl. Phys. Lett.* **2008**, *92*, 191901.
[317] M. Hütter, P. J. in't Veld, G. C. Rutledge, *Polymer* **2006**, *47*, 5494 – 5504.
[318] H. D. Keith, F. J. Padden, Jr., B. Lotz, J. C. Wittmann, *Macromolecules* **1989**, *22*, 2230 – 2238.
[319] T. Iwata, Y. Doi, *Macromolecules* **2000**, *33*, 5559 – 5565.
[320] Y. Kikkawa, H. Abe, T. Iwata, Y. Inoue, Y. Doi, *Biomacromolecules* **2002**, *3*, 350 – 356.
[321] Yu. O. Punin in *Growth of Crystals*, Vol. 14, Consultants Bureau, New York, **1983**, pp. 121 – 131.
[322] Yu. O. Punin, *J. Struct. Chem.* **1994**, *35*, 616 – 624.
[323] P. Ball, *The Self-Made Tapestry, Patterns Formation in Nature*, Oxford University Press, Oxford, Great Britain, **2001**.
[324] C. J. Lee, T. J. Lee, J. Park, *Chem. Phys. Lett.* **2001**, *340*, 413 – 418.
[325] S. Motojima, S. Ueno, T. Hattori, K. Goto, *Appl. Phys. Lett.* **1989**, *54*, 1001 – 1003.
[326] H.-F. Zhang, C.-M. Wang, E. C. Buck, L.-S. Wang, *Nano Lett.* **2003**, *3*, 577 – 580.
[327] D. N. McIlroy, D. Zhang, Y. Kranov, *Appl. Phys. Lett.* **2001**, *79*, 1540 – 1542.
[328] S.-H. Yu, H. Cölfen, K. Tauer, M. Antonietti, *Nat. Mater.* **2005**, *4*, 51 – 55.
[329] S.-H. Yu, M. Antonietti, H. Cölfen, J. Hartmann, *Nano Lett.* **2003**, *3*, 379 – 382.
[330] H. Cölfen, L. Qi, Y. Mastal, L. Börger, *Cryst. Growth Des.* **2002**, *2*, 191 – 196.
[331] H. Cölfen, S. Mann, *Angew. Chem.* **2003**, *115*, 2452 – 2468; *Angew. Chem. Int. Ed.* **2003**, *42*, 2350 – 2365.
[332] J. D. Hopwood, S. Mann, *Chem. Mater.* **1997**, *9*, 1819 – 1828.
[333] M. Li, S. Mann, *Langmuir* **2000**, *16*, 7088 – 7094.
[334] O. Giraldo, S. L. Brock, M. Marquez, S. L. Suib, H. Hillhouse, M. Tsapatsis, *Nature* **2000**, *405*, 38.
[335] O. Giraldo, M. Marquez, S. L. Brock, S. L. Suib, H. Hillhouse, M. Tsapatsis, *J. Am. Chem. Soc.* **2000**, *122*, 12158 – 12163.
[336] L. A. Gower, D. A. Tirrell, *J. Cryst. Growth* **1998**, *191*, 153 – 160.
[337] J. M. García-Ruiz, *J. Cryst. Growth* **1985**, *73*, 251 – 262.
[338] T. Terada, S. Yamabi, H. Imai, *J. Cryst. Growth* **2003**, *253*, 435 – 444.
[339] J. M. García-Ruiz, J. L. Amorós, *J. Cryst. Growth* **1981**, *55*, 379 – 383.
[340] E. Bittarello, D. Aquilano, *Eur. J. Mineral.* **2007**, *19*, 345 – 351.
[341] J.-H. Zhu, S.-H. Yu, A.-W. Xu, H. Cölfen, *Chem. Commun.* **2009**, 1106 – 1108.
[342] E. Bittarello, F. R. Massaro, D. Aquilano, *J. Cryst. Growth* **2010**, *312*, 402 – 412.
[343] J. M. García-Ruiz, E. Melero-Garcia, S. T. Hyde, *Science* **2009**, *323*, 362 – 365.
[344] J. M. García-Ruiz, *Origins Life Evol. Biospheres* **1994**, *24*, 451 – 467.
[345] M. Kellermeier, E. Melero-Garcia, F. Glaab, J. Eiblmeier, L. Kienle, R. Rachel, W. Kunz, J. M. Garcia-Ruiz, *Chem. Eur. J.* **2012**, *18*, 2272 – 2282.
[346] N. Sánchez-Puig, E. Guerra-Flores, F. López-Sánchez, P. A. Juarez-Espinoza, R. Ruiz-Arellano, R. González-Muñoz, R. Arreguín-Espinosa, A. Moreno, *J. Mater. Sci.* **2012**, *47*, 2943 – 2950.
[347] J. M. García-Ruiz, S. T. Hyde, A. M. Carnerup, A. G. Christy, M. J. Van Kranendonk, N. J. Welham, *Science* **2003**, *302*, 1194 – 1197.
[348] L. Addadi, S. Raz, S. Weiner, *Adv. Mater.* **2003**, *15*, 959 – 970.
[349] Q. S. Huo, D. Y. Zhao, J. L. Feng, K. Weston, S. K. Buratto, G. D. Stucky, S. Schacht, F. Schüth, *Adv. Mater.* **1997**, *9*, 974 – 978.
[350] H. Yang, G. A. Ozin, C. T. Kresge, *Adv. Mater.* **1998**, *10*, 883 – 887.
[351] S. M. Yang, I. Sokolov, N. Coombs, C. T. Kresge, G. A. Ozin, *Adv. Mater.* **1999**, *11*, 1427 – 1431.
[352] W.-J. Kim, S.-M. Yang, *Adv. Mater.* **2001**, *13*, 1191 – 1195.
[353] J. H. Jung, H. Kobayashi, M. Masuda, T. Shimizu, S. Shinkai, *J. Am. Chem. Soc.* **2001**, *123*, 8785 – 8789.
[354] S. Yang, X. Chen, S. Motojima, *Appl. Phys. Lett.* **2002**, *81*, 3567 – 3569.
[355] A. M. Seddon, H. M. Patel, S. L. Burkett, S. Mann, *Angew. Chem.* **2002**, *114*, 3114 – 3117; *Angew. Chem. Int. Ed.* **2002**, *41*, 2988 – 2991.
[356] Y. Yang, M. Suzuki, S. Owa, H. Shirai, K. Hanabusa, *Chem. Commun.* **2005**, 4462 – 4464.
[357] S. Iijima, *Nature* **1991**, *354*, 56 – 58.
[358] T. W. Ebbesen, P. M. Ajayan, *Nature* **1992**, *358*, 220 – 222.
[359] S. Amelinckx, D. Bernaerts, X. B. Zhang, G. Van Tendeloo, J. Van Landuyt, *Science* **1995**, *267*, 1334 – 1338.
[360] L. M. Viculis, J. J. Mack, R. B. Kaner, *Science* **2003**, *299*, 1361.
[361] O. Zhou, R. M. Fleming, D. W. Murphy, C. H. Chen, R. C. Haddon, A. P. Ramirez, S. H. Glarum, *Science* **1994**, *263*, 1744 – 1747.
[362] N. G. Chopra, L. X. Benedict, V. H. Crespi, M. L. Cohen, S. G. Louie, A. Zettl, *Nature* **1995**, *377*, 135 – 138.
[363] C.-H. Kiang, W. A. Goddard III, R. Beyers, S. D. Bethune, *J. Chem. Phys.* **1996**, *100*, 3749 – 3752.
[364] M.-F. Yu, T. Kowalewski, R. S. Ruoff, *Phys. Rev. Lett.* **2001**, *86*, 87 – 90.
[365] M.-F. Yu, M. J. Dyer, J. Chen, D. Qian, W. K. Liu, R. S. Ruoff, *Phys. Rev. B* **2001**, *64*, 241403.
[366] S. Amelinckx, X. B. Zhang, D. Bernaerts, X. F. Zhang, V. Ivanov, J. B. Nagy, *Science* **1994**, *265*, 635 – 639.
[367] R. Tenne, C. N. R. Rao, *Philos. Trans. R. Soc. London Ser. A* **2004**, *362*, 2099 – 2125.
[368] A. L. Ivanovskii, *Russ. Chem. Rev.* **2002**, *71*, 175 – 194.
[369] C. N. R. Rao, M. Nath, *Dalton Trans.* **2003**, 1 – 24.
[370] M. Remškar, *Adv. Mater.* **2004**, *16*, 1497 – 1504.

[371] M. Remškar, *Molecular- and Nano-Tubes* (Eds.: O. Hayden, K. Nielsch), Springer, New York, **2011**, pp. 391 – 412.
[372] K. Yada, *Acta Crystallogr. Sect. A* **1971**, *27*, 659 – 664.
[373] S. V. Krivovichev, *Minerals as Advanced Materials I* (Ed.: S. V. Krivovichev), Springer, Berlin, Heidelberg, **2008**, pp. 179 – 191.
[374] V. Yu. Kolosov, C. L. Schwamm, R. V. Gainutdinov, A. L. Tolstikhina, *J. Phys. Conf. Ser.* **2008**, *100*, 082037.
[375] V. Yu. Kolosov, K. L. Shvamm, R. V. Gainutdinov, A. L. Tolstikhina, *Bull. Russ. Acad. Sci. Phys.* **2007**, *71*, 1442 – 1446.
[376] V. Yu. Kolosov, A. R. Thölén, *Acta Mater.* **2000**, *48*, 1829 – 1840.
[377] A. G. Bagmut, V. A. Zhuchkov, V. Yu. Kolosov, V. M. Kosevich, D. V. Melnichenko, *Crystallogr. Rep.* **2006**, *51*, S150 – S157.
[378] A. G. Bagmut, S. N. Grigorov, V. A. Zhuchkov, V. Yu. Kolosov, V. M. Kosevich, D. V. Mel'nichenko, *Russ. Phys. J.* **2007**, *50*, 1071 – 1078.
[379] V. Yu. Kolosov, C. L. Schwamm, J. W. Steeds, *J. Phys. Conf. Ser.* **2008**, *100*, 082038.
[380] V. Yu. Kolosov, L. M. Veretennikov, Yu. B. Starseva, C. L. Schwamm, *Semiconductors* **2005**, *39*, 955 – 959.
[381] V. Yu. Kolosov, A. V. Kozhin, L. M. Veretennikov, C. L. Schwamm, *EMC 2008*, Vol. 2 (Eds.: S. Richter, A. Schwedt), Springer, Berlin, **2008**, pp. 343 – 344.
[382] V. Yu. Kolosov, *EMC 2008*, Vol. 2 (Eds.: S. Richter, A. Schwedt), Springer, Berlin, **2008**, pp. 657 – 658.
[383] M. Kléman, *Adv. Phys.* **1989**, *38*, 605 – 667.
[384] M. J. Bowick, L. Giomi, *Adv. Phys.* **2009**, *58*, 449 – 563.
[385] B. Kahr, J. M. McBride, *Angew. Chem.* **1992**, *104*, 1 – 28; *Angew. Chem. Int. Ed. Engl.* **1992**, *31*, 1 – 26.
[386] B. Kahr, R. W. Gurney, *Chem. Rev.* **2001**, *101*, 893 – 951.
[387] W. L. Bragg, *Proc. R. Soc. London* **1913**, *89*, 248 – 277.
[388] W. H. Bragg, W. L. Bragg, *Proc. R. Soc. London* **1913**, *89*, 277 – 291.
[389] a) M. Kuhnert-Brandstätter, E. Junger, A. Kopfler, *Microchem. J.* **1965**, *9*, 105 – 133; b) M. Kuhnert-Brandstätter, P. Gasser, P. D. Lark, R. Linder, G. Kramer, *Microchem. J.* **1972**, *17*, 791 – 738.
[390] W. L. Noorduin, A. Grinthal, L. Mahadevan, J. A. Aizenberg, *Science* **2013**, *340*, 832 – 837.